Design of Capacitive Micromachined Ultrasonic Transducers for Application in Electronic Travel Aid for the Blind

Revathy A L

A Dissertation Submitted to

Indian Institute of Technology Hyderabad

In Partial Fulfillment of the Requirements for

The Degree of Master of Technology

भारतीय प्रौद्योगिकी संस्थान हैदराबाद

Indian Institute of Technology Hyderabad

Department of Electrical Engineering

19th June, 2012

Declaration

I declare that this written submission represents my ideas in my own words, and where others' ideas or words have been included, I have adequately cited and referenced the original sources. I also declare that I have adhered to all principles of academic honesty and integrity and have not misrepresented or fabricated or falsified any idea/data/fact/source in my submission. I understand that any violation of the above will be a cause for disciplinary action by the Institute and can also evoke penal action from the sources that have thus not been properly cited, or from whom proper permission has not been taken when needed.

REVATHY A L
EE10M08

Approval Sheet

This thesis entitled DESIGN OF CAPACITIVE MICROMACHINED ULTRASONIC TRANSDUCERS FOR APPLICATION IN ELECTRONIC TRAVEL AID FOR THE BLIND   by Revathy A L is approved for the degree of Master of Technology from IIT Hyderabad.

Ketan Detroja
-Name and affiliation-
Examiner

_____
-Name and affiliation-
Examiner

Ashu deb Dutta
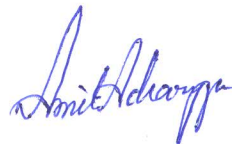-Name and affiliation-
Adviser

_____
-Name and affiliation-
Co-Adviser

Ashok Kr. Pandey
-Name and affiliation-
Chairman

AMIT ACHARYYA
-NAME & AFFILIATION-
EXAMINER

Acknowledgements

It gives me immense pleasure in expressing my gratitude to my advisors Dr. Ashudeb Dutta and Dr. Shiv Govind Singh for their sincere technical and moral support during all phases of the project. Their continuous guidance and motivation have been an inspiration throughout the project. I would also like to thank Dr. B.Venkatesham, Dept. of Mechanical Engineering for having spent his valuable time in guiding me with issues related to acoustics.

I owe my special thanks to Mr. A R Aravinth Kumar for having patiently helped me resolve all software related issues, Mr. Santanam for having helped with the design of electrical circuit, the Microelectronics & VLSI research scholars for extending help in solving various technical problems encountered during the course of the project.

I owe my special thanks to my friends for their unwavering support and for instilling confidence during the project. My loving thanks to my family for their complete patience, encouragement, love and support.

Abstract:

A low cost, compact Capacitive Micromachined Ultrasonic Transducer (CMUT) based Electronic Travel Aid (ETA) to identify obstacle has been proposed. The aim is to enable free movement of the blind in an environment ridden with stationary obstacles with a target distance of 1-2m. In the present work, SU-8 has been chosen as the membrane material of the CMUT. This has enabled drastic reduction in the DC operating voltage to just 22V- an essential limit for handheld devices to be carried by the user. The CMUT is designed to operate at around 70kHz which minimises frequency dependent loss in air. The simulations are carried out in CoventorWare and COMSOL. The results show that on superimposing an AC of 0.5V on the DC, displacements as large as the gap distance of 5um are obtained resulting in output pressures of 140dB on surface of CMUT. On travelling a to and fro distance of 2m, this pressure drops to about 1uPa. To be able to sense this small pressure, a receiver with thin membrane is designed. A circuit has been implemented off chip to process the received signal and generate a PWM signal to drive the vibrator.

Contents

Chapter 1

1. Introduction

1.1   Motivation

Electronic travel aids (ETA) are employed to aid the blind during their movement in an obstacle ridden environment like while walking in the road, when they enter a new building etc. The ability to travel even short distances without help from another person is a great achievement for such people. Usually, through exercise of considerable effort and time, they train themselves about location of objects in their home, school etc. This self-training enables them to walk around effortlessly in these places. But the situation is different when they enter a new building like an office, doctor shop etc. Without aid from a sighted person, it becomes difficult for them to find their way in this new environment. Moreover, several of the developed ETAs are expensive or not user friendly.

Through this project, the aim is to develop an efficient, cost affordable, compact ETA which meets the safe guidance and aesthetic needs of the user during his movement in an unfamiliar building. To meet the aesthetic needs, capacitive micromachined ultrasonic transducers (CMUT) are proposed so that they can be incorporated in the glasses the user wears. The control and processing circuitry can also be built in the same substrate as the MEMS device making the whole device very compact. To meet the safe guidance needs, these ultrasonic transducers are planned to be placed in the glasses to provide information of obstacles ahead of the user, as wrist bands to provide information about obstacles to the side of the user and laser sensors in the shoes to provide information about low lying obstacles. These can help completely eliminate use of the cane. The user can then be informed about the obstacles using electrostatic actuation signals or through vibration signals. The motivation is thus to enable the blind walk independently and confidently by developing a device addressing the above needs.

1.2   Brief Overview of the Thesis

The entire project of development of the ETA can be divided into various design phases:

design of MEMS transmitter, design of MEMS receiver, design of processing circuitry, design of actuation device and circuit. The foremost research topic thus focuses on the design of capacitive micromachined ultrasonic transducers (CMUT) separately for transmission and reception. This thesis presents the design of the transducer for ranging application covering distances of 1-2m and proposes a circuit that can be used for processing of received signal which contains distance information.

Various issues related to design of CMUT are identified and later design of CMUT is carried out to address these issues. CMUT design has involved identifying the frequency of operation, material to be used for the membrane and arriving at device dimensions to suit the above choices. Through simulations carried out using CoventorWare package, Su8 is decided as membrane material suitable for the present application. The device dimensions for the transmitter are chosen for operation at required frequency of around 50kHz. Depending on pressure output from the transmitter as obtained through simulations in COMSOL, the received pressure after various losses in the atmosphere is calculated. The receiver design is later carried out to ensure detection of the very small amplitude received signals. To obtain an approximate idea of the current produced in the receiver in response to the received ultrasound signal, simulation results from CoventorWare and MATLAB are used. All these results validate that the CMUT can be used for application in an ETA for indoor navigation of the blind user. The fabrication steps for transmitter fabrication have been identified and masks for the same are designed using Ledit software.

A circuit for processing the received signal and to obtain distance information is proposed. The idea is to use a counter to obtain the distance information and then generating a corresponding PWM signal to drive the vibrator. The vibration intensity depends on the width of the PWM signal thus conveying distance information to the user. The circuit is tested off chip using peizoelectric transducers.

1.3 Contribution of the Thesis

• Survey of the Electronic Travel Aids developed till date and proposal of new travel aid for reliable guidance during indoor navigation for the blind.

• Literature survey of CMUTs, their fabrication methods, various simulations carried out using FEM and some important results

• Identification of a new material for use in CMUT using simulations

• Provides proof of concept using simulation results from CoventorWare and COMSOL for application of CMUT in ETA for indoor navigation.

• Identification of fabrication steps to fabricate the transmitter

- Provides proof of concept of a circuit that can be incorporated in the same substrate as the MEMS device for providing distance information to the user.

1.4   Thesis Organisation

The entire thesis is organised into nine chapters. Chapter 1 describes the motivation for the project and a brief overview of the entire project. Chapter 2 provides details about the many electronic travel aids developed till date and puts forth a proposal for a new, compact ETA in the form of glasses the user wears. Chapter 3 describes in detail the operation of CMUT, its mathematical analysis, fabrication technologies, techniques proposed for integration of CMUT with electronic circuitry and simulation results presented in literature. Chapter 4 provides theory behind identification of the right material for a particular MEMS application. Chapter 5 contains simulation results which have helped in choosing a circular shape for the membrane and Su-8 as material for membrane of CMUT. Chapter 6 and 7 contain the design of transmitter and receiver respectively carried out by considering the various issues involved in application of CMUT in ETA. Simulation results of these CMUTs carried out using CoventorWare, COMSOL and MATLAB that validate the use of CMUT in ETA for 1-2m range are also presented. Chapter 8 describes the steps intended to be carried out for fabrication of an array of transmitters and also the layouts of masks designed using Ledit. Chapter 9 describes the circuit designed to generate a PWM signal to drive a vibrator that conveys distance information to the user.

Chapter 2

2.   A New ETA for the Blind

Millions of people in India are visually impaired and suffer from either complete or partial blindness. Commuting in the real world ridden with stationary and moving objects is a difficult task for them. The traditionally used white cane provides some guidance by indicating presence of obstacle in his way. This coupled with his hearing sense enables him to walk around, although not at all safely. Many electronic travel aids have been developed which aim to provide complete assistance to the blind. But most of them have disadvantages in terms of their complexity to use them, cost, size etc.

The ETAs typically use ultrasonic waves for obstacle detection as their operation is independent of color and type of material of the object being detected, presence of light, smoke, dust etc. Some also use lasers for sensing. One or more sensors are used per ETA depending on the range and angle to be covered around the user. The distance of the object is calculated based on time taken for ultrasonic waves to reach back at the receiver. This information is then conveyed to the user either in the form of vibrations, audio or speech signals. Some ETAs provide additional features like automatic guidance across obstacles, providing a 2D output, Global Positioning System etc. Training is later provided for proper use of the ETA.

The chapter provides details about some ETAs implemented till date, proposal for a new ETA, its desired application and implementation.

2.1   Literature Survey

The challenge in designing an ETA does not lie in developing a sophisticated detection circuitry but in conveying the obtained information reliably and efficiently to the user and making the device affordable. Many ETAs have been developed over the last several years to act as an electronic replacement for the traditionally used white cane. A brief idea of some of these ETAs is as follows.

The *Ultracane* [1] was developed taking inspiration from the way bats navigate by emitting ultrasonics and provided tactile outputs. It has ultrasonic sensors which provide information about obstacles in the path and those at head height thus enabling the user to obtain spatial awareness about the environment around him. It also provides a range of

settings which help the user set differing distances for obstacle detection according to his needs.

Dr.Kay developed a *Sonic Cane* [2] which was a torch emitting ultrasonics providing audio outputs. It could be used either independently or by attaching the torch to a cane. The torch scans the environment around the user to provide information about obstacles. Later he also developed a *Sonic Guide* which consisted of a pair of spectacles providing binaural output. On the spectacles, one ultrasonic transmitter and two receivers (one to the left and other to the right with an overlap at the centre of the glasses) were mounted to provide distance and directional information.

Another popular ETA is the *Laser Cane* [3] which has a long history of development. Newer versions of this cane were produced by working on shortcomings in the previous versions. It uses infrared for sensing by emitting three beams. One beam is to indicate the user of levels lower than surface by 6 inch when they're around 6ft away from user. The other beam is to detect objects straight ahead to the user covering a distance of about 5ft to 12ft. The third which is an upward looking beam is for objects located at head height. The advantage of using three beams is that it reduces the beamwidth of each beam emitted.

Later ETAs with *obstacle avoidance algorithms*, used in the field of mobile robotics, were developed thus increasing the level of technology built into an ETA. They provided active guidance to the user i.e. they guided the user in a predefined direction. *NavBelt* [4] and *GuideCane* [5] fall in this category. The NavBelt provides binaural feedback indicating the suggested direction of travel. This device is worn around the waist and it consists of two arrays of 8 sensors each, with each array covering 120degree sector. The Guide Cane is a cane that rolls over wheels over which an array of ultrasonic sensors is mounted. It has a miniature joystick which the user uses to specify direction of travel and the cane guides the user in that direction. The sensors detect obstacles in 120° sector ahead of the user. On detecting an object, an on-board computer uses an obstacle avoidance algorithm and causes the wheels of the cane to rotate and guide the user past the obstacle. It then resumes its original direction of travel. It also provides for detection of up steps and down steps. They however did not gain wide acceptance because of their huge size and cost.

The *Sonic Pathfinder* [6] was another device which has artificial intelligence built into it in that objects at a constant or increasing distance are ignored. It is an ultrasonic device with two transmitting and three receiving transducers mounted on a head band. The auditory signal that alerts the traveller to objects in the path corresponds to eight notes on the musical scale analogous to distance, highest note for far away object.

The conventional long cane provides information about objects only at leg height of the user. To provide information about the forward path at chest and head height of the user and act as a supplement to the cane, a device called *The Wheelchair Pathfinder* [7] was devised. It is a device that can be mounted on a mobility vehicle or wheelchair. It uses a mix of IR and ultrasonic sensing providing a good amount of information in the form of vibrations or beeps. The disadvantage is that every blind person may not wish to sit on a wheelchair and commute.

The more advanced ETAs built today use stereo vision cameras which provide 3D information about the surrounding environment. This information when conveyed to the user helps him form a mental map of the object, thus enabling him walk quickly in an obstacle ridden environment. Examples are the *vOICe* [9] and *Intelligent Glasses* [10]. The vOICe involves three components: sunglasses with a miniature camera, software that translates images into different audio stimuli, and headphones for the user. Using volume, frequency, stereo, and other audio variables, the local environment is represented to the blind individual as a "soundscape" through the headphones. The image from camera is sent to a computer. Software in the computer scans each image from left to right converting each pixel into a beep with frequency representing vertical position and volume, the brightness. This sound information is decoded in auditory cortex of brain. It is seen that after 10 to 15 hours of training the visual cortex lights up and helps in better understanding of soundscapes.

The Intelligent Glasses [10] is a man machine interface integrating computer vision with human tactile senses. The system consists of a stereo vision camera that acquires, encodes and transmits the environment's representation to a scene analyser module. Vision algorithms are then applied in order to identify obstacles which is then converted into a tactile domain and displayed on a tactile interface for use by the visually impaired. The above two devices consume a lot of processing power and are expensive. They may also not be reliable when objects are moving if processing speed is not high.

In [11], a wearable travel aid in the form of a coat is presented. Two ultrasound transducers are used, one as a transmitter and the other as a receiver. A microcontroller gathers information from the transducers in the form of PWM pulses, the width of which gives distance information. This is converted to a voltage to drive the vibrators. Two vibrators are used on left and right side of the coat. Directional information of the obstacle is obtained by actuating the appropriate vibrator.

Many new technologies use GPS, WiMax, RFID for providing guidance to the blind user [12]- [17]- [18].

Table 2.1 summarises the above mentioned devices.

Name of the device	Target	Output type	Inventor
Batcane	Distance	Vibration	Sound Foresight and Cambridge Consultants
Bat 'K' sensor	Distance	Audio patterns	Bay Advanced Technologies Ltd
Laser cane	Distance	Vibration,sound	J. Malvern Benjamin
Guide cane	Distance	Automatic guidance in predefined direction	Johann Borenstein University of Michigan
Nav Belt	Distance	Binaural audio	Johann Borenstein and Iwan Ulrich, University of Michigan
Miniguide	Distance	Vibration	Greg Phillips
Sonic Guide	Distance	Audio	Dr. Kay
NOD	Distance	Musical tone	
Wheelchair pathfinder	Distance	Beeps	Nurion Raycal, USA.
Sonic pathfinder	Distance	Musical notes	
vOICe	image data	Stereophonic audio	Peter Meijer
Intelligent glasses	image data	2D array of vibrators	Ramiro Velázquez, Flavien Maingreaud and Edwige E. Pissaloux

Table 2.1: Summary of some ETAs developed till date

2.2 Proposal

The ability of a blind person to travel even short distances successfully without the aid of a sighted companion is a challenge. On self-training, the blind usually acquaints himself to the environment frequently visited by him like his home, school or workplace. But when he visits a new building like doctor shop, a government office etc, he finds it difficult to find his way to the desired place. The aim of the present project is thus to develop ETA to enable safe movement in an unknown place by detecting stationary obstacles over distances of 1-2m. The proposed implementation of such an ETA is shown below and described in the next sections.

Obstacle detection ahead of the user using MEMS transducers

Obstacle detection on sides of the user

RFID reader which guides user to destination room

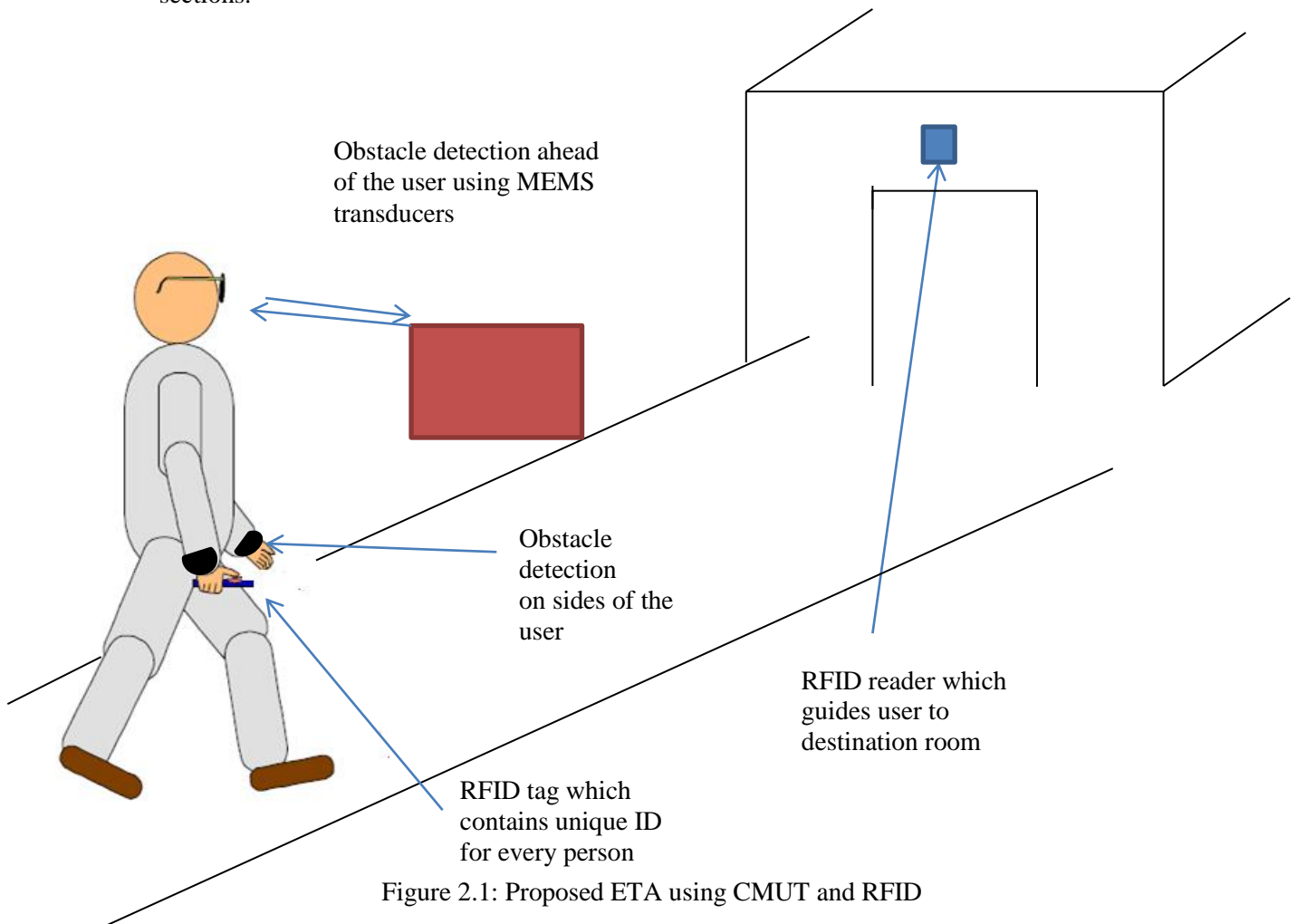RFID tag which contains unique ID for every person

Figure 2.1: Proposed ETA using CMUT and RFID

2.2.1 Sensor Implementation

The objective of this project is to implement ultrasonic sensors in the glasses which the blind wear with a hope to avoid use of cane. These sensors can be incorporated in the glass frame the user wears. With such mounting, the requirement that the device be light and look natural also need to be satisfied. Hence MEMS ultrasound transducers can be fabricated and

used. The sensors on glass can be used to cover the field ahead of the user. To indicate object presence on the sides of the user, these transducers can be worn as wrist bands. Also ultrasonic waves have large wavelengths because of which small objects like curbs, steps, potholes which are important while treading a footpath etc., go undetected. To solve this issue, using multi sensor concept, laser sensors can be incorporated separately in the foot part of the user (not shown in figure). The different location of sensors can be seen in Figure 2.1.

MEMS ultrasonic transducer also called Capacitive Micromachined Ultrasonic Transducer (CMUT) is presently a topic under great research because of wide biomedical and ranging applications of ultrasonics. All the ETAs using ultrasonics developed till date use piezoelectric crystals for generation of ultrasound. A CMUT on the other hand offers many advantages [13]. It offers excellent acoustic impedance matching with air, the surrounding medium. This results in efficient coupling of ultrasound into the air thus providing high dynamic range (around 50dB more than piezoelectric counterpart) and hence high sensitivity for the transducer. Thus even highly attenuated waves to which conventional transducers are insensitive to, can be detected by these transducers increasing reliability of the device. The response of these transducers is determined by the size and shape of membrane used to produce ultrasound by vibrations. Wide range of devices ie short range and long range transducers can be built on the same substrate thus eliminating need for different transducers for different ranges. Also these devices are manufactured using standard IC processes like lithography, deposition etc. This provides possibility of integration of device with supporting electronic circuits. All the above features provide attractive reasons to use CMUT over conventional transducers. The last two features enable making the device compact and lightweight. It also has an added advantage of possibly being a cost effective implementation as it can be manufactured using batch fabrication techniques.

2.2.2 Actuation

Actuation involves conveying information derived about obstacles to the user. This can be done by auditory or tactile means. Auditory output is not desirable as the user might need to use his hearing sense to make his own judgements while walking on the road. Tactile outputs can be in form of vibration, an electric pulse or heat with intensity depending on location of the obstacle. Such methods of providing output are called sensory substitution methods as one human sense receives information that is normally received by another human sense. Stimulation using vibration is widely employed. The hand held part of the cane vibrates with certain intensity depending on distance of the object from the user.

Heat stimulation can be done if the actuator can heat and cool down appropriately in a short time. Tactile stimulation using electric pulses is called electrotactile stimulation where a tactile sense is evoked within the skin at the location of the electrode by passing electric current through the skin.

As seen in the earlier table, vibration is used in many ETAs like Ultracane, Laser Cane etc. ETAs with electrotactile simulation have also been developed. Great amount of work on conveying information obtained from a non-tactile source such as camera to a 2D matrix of electrotactile actuators placed on the skin is being carried out. This information is converted to an encoded pattern which excites selective actuators through application of painless currents. There are various positions of the human skin where electrotactile electrodes can be placed like tongue, fingertip, lip, forehead etc. In [15], the 2 point discrimination threshold voltage and sensing limits of these various skin surfaces are listed. Tongue has highest sensitivity and least threshold followed next by the fingertip. In this paper, a selective stimulation haptic display using a display glove is reported where 5 stimulating points are located one each on root of the corresponding finger. A particular point is stimulated based on distance information. In [16], receptive characteristics of the fingertip for varying sizes of electrodes, distances between electrodes and stimulation frequency is investigated. It was found that size of electrodes and stimulation frequency did not affect a person's ability to recognise location of electrotactile stimuli. The idea thus is to exploit sensitivity of fingertip by placing one electrode on each fingertip and exciting a combination of these based on distance and location of object.

The objective of this project is to use vibration mechanism for actuation. A vibrator is a DC motor with an unbalanced load over it. Normal motors are well balanced and do not cause any vibrations. With an unbalanced load, there will be vibrators due to rotation of the motor. Higher the speed of rotation, higher is the vibration. The speed of the motor can be controlled using a PWM pulse. Thus a circuit needs to be designed to generate a vibration proportional to the distance of the obstacle detected.

2.2.3 RFID:

While MEMS transducers are used for obstacle detection, RFID is used for localization of the user. It is included with the intention of making the user completely independent by providing information about his current location and then guiding him appropriately to the right room. It is developed widely in the US and European countries to assist in indoor navigation of the blind. In [17], one such indoor navigation system is proposed where a number of passive tags containing tag location are incorporated along various tracks in the building. A reader reads information from the tag, sends it to a

microcontroller unit which then communicates with the navigation server. This server provides a route which the user can use to reach his destination. Users may sometimes change their route, hence a new route is again sent back to the user. In [18], an RFID system is designed for object identification in a building and also for path finding. Tags are mounted on various objects and for path finding, a grid of tags is used. A hand mounted reader gets information from the tags and sends it to the server using the zigbee module. From the server, an audio file is retrieved and this is sent to the user on the FM band. This file contains information about the obstacle or route information depending on route entered. Many more such systems incorporating RFID can be found in literature.

The motive of including RFID in the ETA is to guide the blind person to the right classroom. The time table will be pre loaded in server and will help in guiding the user to the right classroom. Tags will be carried by the user and the reader will be present at fixed locations.

2.3   Break up of the project

- Design of MEMS ultrasonic transducers
- Development of laser sensors for low level object detection
- Development of processing circuitry in each of the above phases to generate the appropriate actuation signal
- RFID system design
- Integration of the modules to obtain a fully functional device

Chapter 3

3. Theory of CMUT

The design of a transceiver system for ranging is the first phase in the development of the electronic travel aid for the blind. Transceiver design is a multidisciplinary process encompassing transducer element design, array design, consideration of signal propagation characteristics and signal processing of the received sound and sound to be transmitted. The first step is thus the design of a basic transducer element. For this purpose, a MEMS electrostatic transducer, the CMUT is used. This section describes the construction, operation, fabrication and design equations of the CMUT as obtained from the literature.

3.1   Introduction

Ultrasound is conventionally generated by peizoelectric transducers. All the ETAs developed till date and using ultrasound for object detection are based on peizoelectric transducers. An alternative way of generating ultrasound is by using electrostatic transducers. These transducers are in the form of a capacitor with one plate fixed and the other, movable. In order to achieve sufficient sensitivity, high electrostatic forces are required to exist in the gap between the capacitor plates. Electrostatic forces are inversely proportional to the square of distance between the charged plates. This means that transducers with sub-micron gaps are required to operate efficiently. With the development of MEMS technology which uses CMOS compatible fabrication process to fabricate these micro devices, it became possible for the realization of electrostatic ultrasonic transducers with sub-micron gaps. These transducers came to be called 'Capacitive Micromachined Ultrasonic Transducers'.

These CMUTs have many advantages compared to the traditionally used peizoelectric transducers [19]. They are listed below.

- Peizoelectric transducers are not suitable for use in air because of high impedance mismatch between peizoelectric and air. The acoustic impedance of air is 400 Rayls while that of peizoelectric is around 30MRayls making them very inefficient. With a cMUT, better match can be obtained.

- Matching layers are placed between peizoelectric and air to improve matching but availability of materials to take care of this large impedance mismatch is difficult. Also this matching comes at the expense of bandwidth.

- A peizoelectric's frequency range is determined by its geometry. Sometimes the size may not converge to a realizable configuration for that frequency.

- They depole at temperatures around 80^0C preventing them from being used at high temperatures, a consideration for testing applications.

The above disadvantages make CMUT a highly attractive option for efficient ultrasound generation. Also since they are fabricated using well established CMOS processes, they also provide the opportunity of integration of electronic circuitry with the device either monolithically or in the form of a 3D IC. It also allows for batch fabrication, hence low cost for the transducers is acheivable.

3.2   CMUT Construction and Operation

A CMUT consists of a fixed and a movable electrode. MEMS devices are constructed over a silicon substrate which acts as the base over which the device operates. Likewise, a CMUT consists of a silicon substrate which acts as the ground electrode. A metal layer can also be deposited over this substrate to act as the ground electrode. This acts as the fixed electrode of the CMUT. A membrane of dielectric material like silicon nitride is suspended at a certain height from the substrate. Vacuum is maintained in the gap between the ground electrode and the membrane. A metal electrode is deposited over this membrane to act as top electrode. This acts the movable electrode. The cross section of a single CMUT is as shown below.
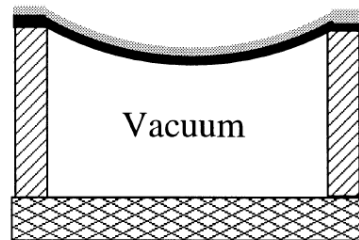

Figure 3.1: cross section of a single CMUT [19]

When a DC voltage is applied between the top and ground electrodes of the transducer, electrostatic forces are developed between the plates of the capacitor which results in deflection of membrane towards the fixed electrode. This deflection is resisted by the stiffness of the membrane. The amount of deflection is proportional to the applied DC voltage. Also, for the same DC, deflection is much greater in the case of smaller gaps. When an AC voltage with a frequency in the range of ultrasound is applied over the deflected membrane, the vibrations of the membrane result in the generation of ultrasound at that

particular frequency. The device is operated with DC applied as it increases the sensitivity of the device.

3.3   Mathematical Analysis of Device Operation

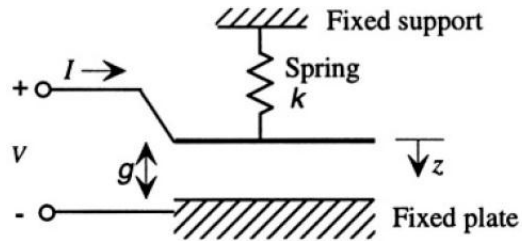The transducer can be represented as shown below:

Figure 3.2: Transducer representation [20]

Here the transducer is shown to have a fixed plate and a movable plate with a spring constant 'k'. It can thus be considered as a capacitor. The mathematical analysis follows [19]:

When a DC voltage is applied, the force exerted by the capacitor is

$$F_{capacitor} = \frac{\varepsilon S V^2}{2(d_{eff} - x)^2}$$

Eq. 1

where,

$d_{eff} = d_0 + \dfrac{d_m}{\varepsilon_r}$ - the effective gap between the electrodes

d_0 = vacuum gap between electrodes

d_m = thickness of the membrane

S = area of capacitor plates

With DC and AC applied,

$$V^2 = \left(V^2{}_{DC} + 2V_{DC}V_{ac} + V^2{}_{ac}\right)$$

Eq. 2

With the displacement assumed small compared to gap distance, we can neglect 'x term' thus obtaining,

$$F_{capacitor} \propto V^2{}_{DC} + 2V_{DC}V_{ac} + V^2{}_{ac}.$$

21

As seen from the above equation, without DC the frequency of membrane vibration would be twice that of applied frequency.

If we choose $V_{DC} \gg V_{ac}$, then we have $F_{ac} \propto 2V_{DC}V_{ac}$, thus linear analysis on the device can be carried out.

The spring in turn exerts a force given by

$$F_{spring} = -kx$$

The membrane settles with a displacement such that the net force is zero ie,

$$F_{capacitor} = F_{spring}$$

Some of the terms associated with CMUT are described below:

1. Collapse voltage: As the applied DC voltage is increased, there is a point at which the electrostatic force overwhelms the spring force. There is no more restoring force offered by the membrane and it collapses on the substrate. The voltage at which this happens is called collapse voltage or pull in voltage. It is given by,

$$V_{collapse} = \sqrt{\frac{8kd^3_0}{27\varepsilon S}}$$

Eq. 3

with $x_{collapse} = d_0 / 3$

2. Snapback voltage: After the membrane has collapsed, it will not snap back until the voltage is reduced from $V_{collapse}$ to $V_{snapback}$ given by,

$$V_{snapback} = \sqrt{\frac{2kd^2_{insulator}(d_0 - d_{insulator})}{\varepsilon_{insulator}S}}$$

Eq. 4

Where $d_{insulator}$ is the insulating layer deposited over the bottom electrode to prevent shorting after membrane collapse.

3. Electrostatic spring softening: As the DC voltage applied increases, the displacement of the top plate increases and a spring force is developed in the opposite direction. However this plate displacement further increases the electrostatic force resulting in more displacement. This increase can be interpreted as spring softening. This dependence of 'k' on DC voltage is given by,

$$k_{soft} = k - \frac{\varepsilon S V^2_{DC}}{d_0^{\ 3}}$$

Eq. 5

Next, the equivalent circuit model of the transducer is arrived at as described in [19]. This model is valid under small signal conditions for receiving MUT and for a transmitting MUT as long as the membrane displacement is not near the collapse point. The approach involved is to find the mechanical impedance of the membrane in vacuum and then to insert it in a transformer equivalent circuit. Transformers aid in translating variables from one energy domain to another and here it is used as two port network with one port representing the electrical domain (voltage and current) and the other the mechanical domain (force and velocity).

The mechanical impedance is found using Mason's derivation and introducing some corrections to it. Mechanical impedance is defined as ratio of applied pressure to average velocity of the membrane ie,

$$Z_m = \frac{P}{v_{average}}$$

$v_{average}$ is found by first finding the displacement profile $x(r)$ of the membrane which follows the zeroth order Bessel function distribution ie maximum displacement at centre and zero displacement at the ends of the membrane. The velocity profile $v(r)$ and average velocity $v_{average}$ are then given by,

$$v(r) = j\omega x(r)$$

$$v_{average} = \frac{1}{\pi a^2} \int_0^a \int_0^{2\pi} v(r) r \partial\theta \partial r$$

$$= \frac{jP}{\omega \rho d_m} \left[\frac{2(k_1^2 + k_2^2) J_1(k_1 a) J_1(k_2 a)}{a k_1 k_2 (k_2 J_0(k_1 a) J_1(k_2 a) + k_1 J_1(k_1 a) J_0(k_2 a))} - 1 \right]$$

Where, ω is the frequency of operation

a is the membrane radius

ρ is membrane density

d_m is the membrane thickness

k_1, k_2 are constants depending on Young's modulus E, Poisson's ration σ and tension T of the membrane

Using the above, expression for mechanical impedance is arrived at. The equivalent two port circuit for the MUT can now be drawn as shown below
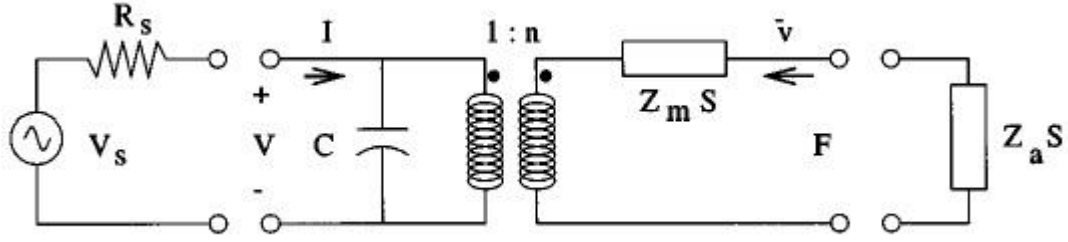
Figure 3.3: equivalent circuit of MUT

where,

V_s, R_s are the source voltage and source resistance respectively

$C(t)$ is the electrical capacitance given by $C(t) = \dfrac{\varepsilon_0 \varepsilon S}{\varepsilon_0 d_m + \varepsilon l_a(t)}$ with $l_a(t)$ being the time

varying gap between the electrodes and ε, the permittivity of the membrane.

n is the transformer turns ratio signifying the transformation of velocity, a mechanical

quantity into an electrical quantity and is given by $n = \dfrac{V_{DC} \varepsilon_0 \varepsilon^2 S}{(\varepsilon_0 d_m + \varepsilon l_a)^2}$

Z_a is the acoustic impedance of the medium into which ultrasound is radiated.

3.4   CMUT Fabrication

Many methods have been proposed in literature for fabrication of CMUT. Two of them are used widely [22] and is described in this section. The first CMUTs were made using sacrificial release process where a sacrificial layer is used to create a gap. Wafer bonding method is a new CMUT fabrication technique and uses a different approach for making the cavity. These two methods are described in detail below.

i.   Sacrificial release process:

The silicon wafer is doped heavily to act as the ground electrode. The process is explained using silicon nitride as the membrane. Silicon nitride is then deposited using LPCVD process. The composition of gases is adjusted to obtain a low stress nitride layer. This layer acts as an etch stop layer protecting silicon wafer from the etchant during the wet sacrificial release process. Then a layer of polysilicon is deposited using LPCVD to act as sacrificial layer. Regions of reduced etch channel are defined to control flow of KOH into cavity during etching. Another layer of polysilicon is then deposited and this decides the thickness of reduced etch channel. This layer is then patterned to define the active area ie the area where cavity will be formed. LPCVD silicon nitride layer of required thickness is then

deposited over the polysilicon and etch holes are defined on this layer. The wafer is immersed in KOH solution. Through these holes, KOH etches the polysilicon layer releasing the membrane. The etchant is selected such that it has high selectivity to the sacrificial layer and not to the membrane layer. The etch holes are then sealed by another deposition step where silicon nitride is deposited. Because silicon nitride is deposited at low pressure, the cavity is considered to contain vacuum. Leaving air in the cavity introduces squeeze film damping and may not be desirable. A metal is deposited over the membrane and then patterned. The electrode coverage determines the electromechanical transformer ratio and parasitic capacitance. The process steps are shown in the diagram below.

(a). substrate doping, etch stop layer deposition, sacrificial layer deposition & patterning

(b). reduced etch channel height regions & formation of active area

(c).membrane   deposition

(d).   etch   hole   definition

(e). membrane release using KOH

(f). vacuum sealing and top electrode   deposition   & patterning
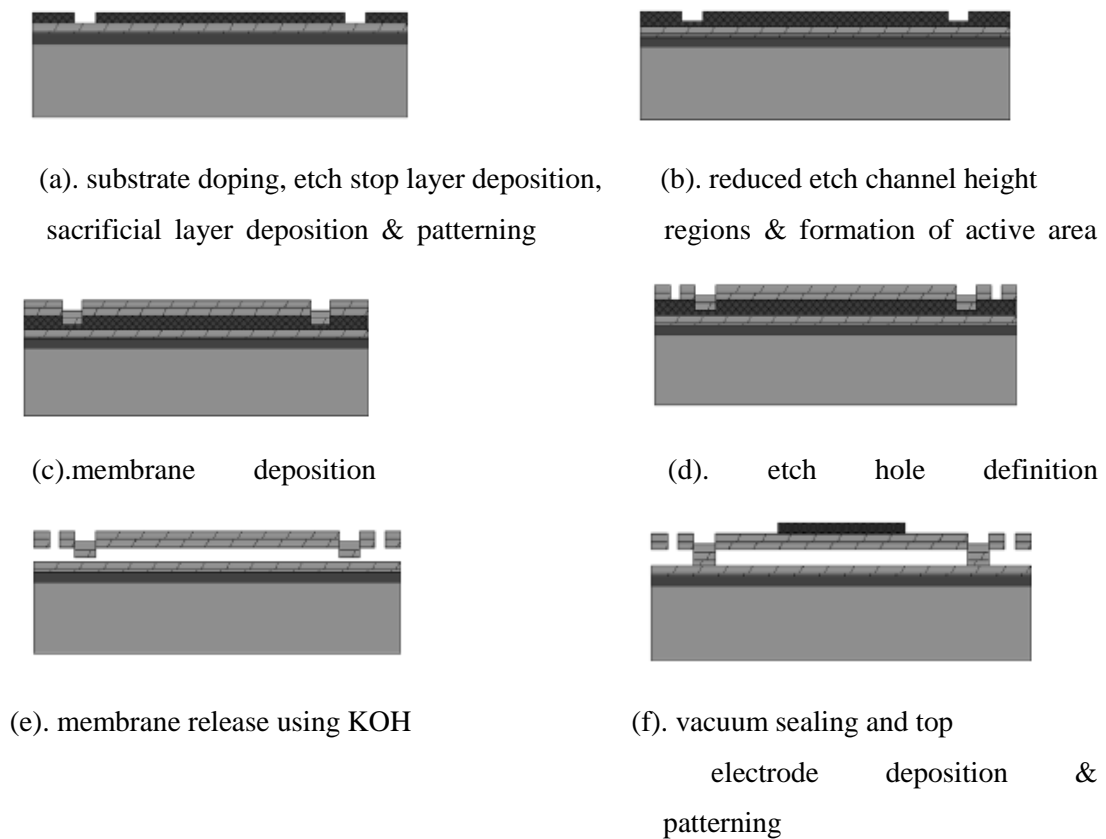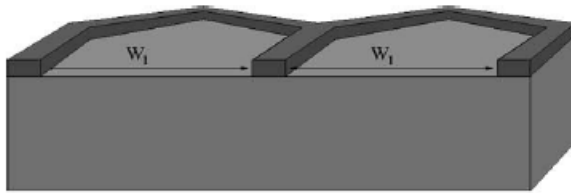
Figure 3.4: steps involved in CMUT fabrication using sacrificial release process
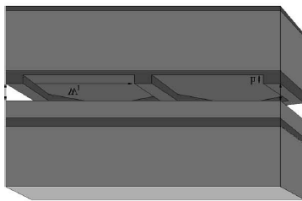
ii. Wafer bonding process:

Wafer bonding is a bulk micromaching process. There are three types of wafer bonding: anodic bonding, fusion bonding and adhesive bonding. Silicon fusion bonding between two silicon surfaces is used to form the CMUT. This bonding takes place at high temperatures resulting in formation of strong covalent bonds between silicon wafers. The fabrication of CMUTs using this process is done with two wafers: a silicon wafer and a SOI wafer. The cavity is defined on the silicon wafer. The silicon wafer is oxidised to a predetermined

thickness and the cavity is defined on this layer in case the cavity height is less than 2um. In case of greater cavity depths required, the cavity is formed in the silicon itself by etching till the required depth. After cavity definition, the silicon wafer and the SOI wafer are brought together in vacuum and at temperatures of around 1100C, strong covalent bonds are formed. After bonding, the handle of the SOI is removed by etching to release the membrane. The process steps are shown in the diagram below.

(a). oxidation and cavity formation

(b). bonding process
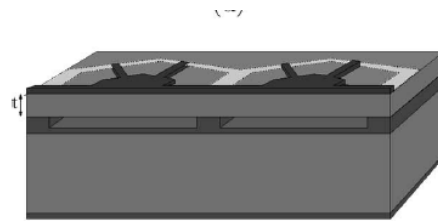
(c). removal of handle, top electrode deposition & patterning

Figure 3.5: steps involved in CMUT fabrication using wafer bonding process

Wafer bonding process reduces the complexity of CMUT fabrication. The number of masks has reduced from six to four and five deposition steps are reduced to two oxidation steps thus reducing the processing time substantially. Also it is possible to optimize membrane and cavity at the same time as they are both defined on different wafers. But these advantages come at the cost of expensive SOI wafers.

The CMUT structure used for various applications is in the form of an array. An array element consists of numerous CMUT cells connected in parallel. A collection of array elements placed side by side forms the array. Such an array is used in medical imaging purposes.
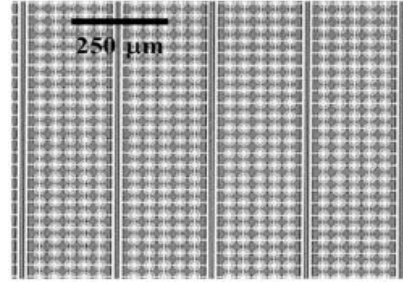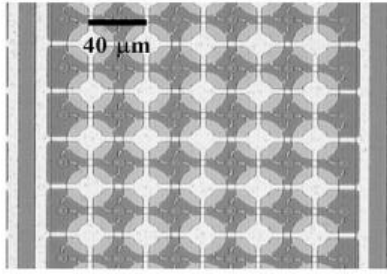
(a): 5 cell wide array element   (b): CMUT array with 4 array elements

Figure 3.6: CMUT array element and array

The CMUTs can be fabricated with membranes of different shapes. Hexagonal and rectangular membranes result in better area optimization when using array of CMUTs. Circular membranes are mainly used for mathematical analysis as they are easier to model, they also yield higher displacements than other membranes.

3.5   Regions of Operation of CMUT

Three different regions of operation for the CMUT are suggested in literature.

1)   Pre collapsed regime: Here the DC voltage applied is less than the collapsed voltage. Hence it more efficient when operated near collapse voltage. The electromechanical coupling coefficient is almost equal to 1 when operated near collapse voltage.

2)   Collapsed regime: Here a DC voltage greater than collapse voltage is applied to collapse the membrane. Now, an AC voltage is applied and it is seen [24] that the sensitivity of the device is much larger than that obtained in pre collapse regime.

3)   Collapse snapback operation: This method of operating the CMUT is suggested in [25]. In this method, the voltage pulses are applied such that the membrane collapses and snaps back thus utilising a larger range of membrane deflections. The output acoustic pressures were found to be much larger than that obtained in previous two cases.

3.6   CMUT Design Equations

The geometry and properties of the membrane material determines the resonant frequency and quality factor of the CMUT. The cavity gap is determined depending on the required pull in voltage. The following are the equations used to obtain the device geometry parameters given resonant frequency and possibly quality factor. These are derived using the plate theory [26].

Resonant frequency,

$$f_0 = \frac{0.47 d_m}{a^2} \sqrt{\frac{E}{\rho\left(1-\sigma^2\right)}}$$ Eq. 6

Quality factor,

$$Q = 1.84 \frac{\rho t}{R_{rad}} \omega_0$$

Eq. 7

where R_{rad} is the radiation resistance of the medium

The gap is determined using expression for collapse voltage given by

$$V_{collapse} = \sqrt{\frac{8kd_0^3}{27\varepsilon S}}$$

where, k is the spring constant for cases when deflection is small compared to membrane's thickness. The spring constant in non-linear for large deflections.

3.7   CMUT Characterisation

Many simulations have been carried out on CMUTs using FEM software packages for the purpose of CMUT characterization, optimizing various parameters etc. Earlier all characterizations were carried out after fabricating the device. With these packages, an optimum CMUT can be designed before it is fabricated. Some of the finite element software packages available for CMUT design are ANSYS, CoventorWare, COMSOL, IntelliSuite etc. An overview of such work found in literature is presented here.

In [27], it is shown through simulations using ANSYS that the performance of the CMUT can be improved by proper patterning of the electrode using the basis that electrostatic force should only be applied only where it is most effective ie in the centre of the membrane. The bandwidth in found to double when electrode area is around 50% of the membrane area. In [28], a pulse echo ultrasound system is modeled. Accurate analytical models for the transmitting CMUT, receiving CMUT and the propagation channel are developed using which plots are obtained for electrical impedance, transmitting sensitivity, receiving sensitivity and are shown to agree well with measured values of the same parameters. In [29], simulations are carried out in ANSYS to compare the performance of optimized CMUT in conventional and collapse mode operations. It is shown that collapse mode operation has very high sensitivity compared to that of conventional mode of operation thus resulting in very much higher output pressures. In [30], static simulation of a CMUT array is carried out using CoventorWare package. The simulations are carried out on CMUTs with different radius, membrane thickness and gap height and results are presented. Initial simulations in CoventorWare related to the project were carried out based on this paper. In [31], simulations are carried out on prestressed models as stress stiffening affects static deflection, resonant frequency, pull in voltage, small signal sensitivity. Simulations

results including stress stiffening are shown to be in good agreement with experimental results. It is also mentioned that transient and harmonic analysis are sufficient to compare between different CMUT designs and that transient simulations are more difficult for CMUTs with large quality factors. In [14], a single CMUT cell with hexagonal membrane is simulated. Hexagonal CMUTs are used so that transducer array can be fabricated at lower cost. It is also mentioned that if the membrane is biased appropriately and subject to ultrasonic waves at resonant frequencies, then large detection currents can be generated. In [15], an analytical model for a CMUT as a coupled system of electrostatics, mechanics and acoustics is developed. The static, harmonic and far field pressure results are compared with FEM simulations carried out using COMSOL and is shown that CMUT behavior can be fairly well approximated using this coupled model.

3.8   Integration of electronics with CMUT Arrays

CMUTs are used extensively in medical imaging applications where high frequency of operation is required. Initial effort was thus in the design of CMUT arrays appropriate for these applications. Next, integration of ultrasonic transducer arrays with data acquisition and signal processing circuitry became important. Different methods of integration have been identified and a few methods tried in literature.

In [34], CMUTs have been integrated with analog switching electronics and have been tested successfully. The CMUTs are made over the CMOS electronics with the transducer bottom electrodes making direct contact with CMOS circuit's metal layer. Tests were conducted to show that the radiation pattern is not affected due to the switching electronics. In [35], a noise optimized CMOS front end circuit for 2D CMUT arrays is presented. A pulser, protection circuit and two topologies of read out amplifier are designed to minimize noise. In [18], an IC which consists of a pulser and a transimpedance amplifier for every array element is flip chip bonded using through wafer interconnects to the CMUT array. A CMUT array is fabricated and every element is provided with an electronic circuit consisting of a pulser, preamplifier, high voltage switch and a logic block that generates control signals and complete characterization of the device is carried out. In [37], CMUT array is integrated with CMOS front end electronics using CMUT-on-CMOS process. Here CMUT elements are built after CMOS fabrication. This single chip integration reduces interconnection complexity. After integration, the successful working of the system with pulse echo measurements is shown.

Chapter 4

4. Materials for MEMS

There are three basic requirements for a material to be used in MEMS devices [38]:

1)   Compatibility with semiconductor fabrication technology

2)   Good electrical as well as mechanical properties

3)   Intrinsic properties that retard development of high stresses during processing

There is an enormous growth of materials that can be used in microfabrication technology. There are four classes of engineering materials that can be used in MEMS devices- metals like Ni, Al, non-metals like Si, Ge, GaAs, polymers like Su8, polyimide and ceramics like diamond, SiC, Si_3N_4, SiO_2 etc. The suitability of a material for a particular application is decided based on certain performance and reliability metrics that consider Young's modulus (E), density (ρ), failure strength (σ_f). Ashby charts are used for this purpose. These charts are plots of material performance indices for frequency, deflection etc., for mechanical elements like plates, beam etc. Some of the material indices (M_i) used are as follows:

$M_1 = E$ corresponds to force to be applied to the device
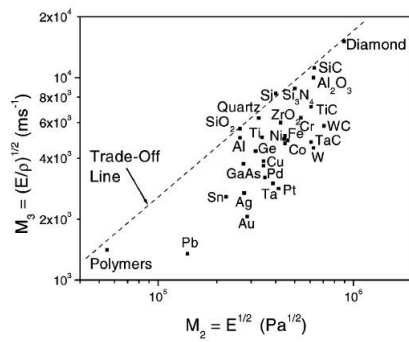
$M_2 = \sqrt{E}$ corresponds to actuation voltage

$M_3 = \sqrt{\dfrac{E}{\rho}}$ corresponds to speed of vibration i.e. frequency of vibration

$M_4 = \dfrac{\sigma_f}{E}$ corresponds to deflection of a beam where σ_f is the fracture strength that is how long the membrane can deflect before it breaks
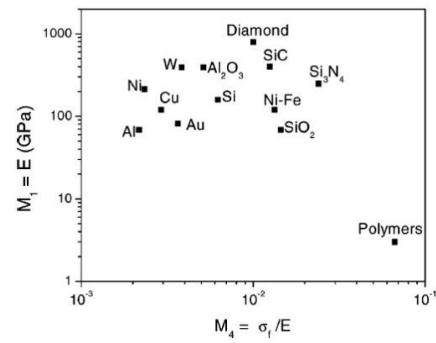
$M_5 = \dfrac{\sigma_f^{3/2}}{E}$ corresponds to deflection of a plate

The following are Ashby charts [39] produced using the above material indices.

(a): speed v/s square root of E   (b): E v/s ratio of fracture strength to E

(top right corner: high speed   (top left corner: large stroke materials)

high actuation voltage)

Figure 4.1: Ashby charts

In case of application to actuators, it is analysed from the above charts in [39]that diamond, alumina, silicon carbide, silicon nitride, silicon are best for high stroke, high speed actuators; polymers for large displacement, low actuation voltage devices.

For a CMUT, material indices M_2, M_3 and M_5 are of concern. Material with low M_2 is required to minimise actuation voltage. Material with high M_3 is required to maximise flexural vibrations of the plate. Material with high M_5 is required to maximise deflection under a particular load. For the present application since high frequency operation is not required, M_3 need not be considered. The best choice thus seems to be polymer as it has high deflections for low actuation voltages.

Chapter 5

5. CMUT Design and Analysis

5.1   Issues related to use of CMUT in ETA

A lot of research is being carried out to develop CMUTs for use in medical imaging and non-destructive testing. All these applications of CMUT proposed till date, are limited to very short distances like millimeters and to imaging applications. Moreover since the electronic equipment used with CMUT in these applications is stationary, it is possible to use high supply voltage equipment to drive the CMUT and obtain high output pressures. But the application of CMUT to travel aid requires that considerable distances be covered during ranging for obstacle detection. Developing such an ultrasound transducer with sufficient transmit range capability and high receive sensitivity in air is a challenge because of rapid attenuation of ultrasound in air. Also the device is to be carried by the blind person, hence high supply voltages cannot be used. The maximum allowed DC voltage that can be carried by a person is 22V. The challenge is thus to use low supply voltages while still maximizing displacement of the membrane of the CMUT. When CMUT is operated in air, the membrane displaces due to atmospheric pressure. Voltages are applied on this displaced membrane to obtain transducer function. Hence large gaps need to be fabricated and the membrane material should have sufficient strength to sustain high displacements especially when used as transmitter.

Simulations are carried out using CoventorWare package on CMUTs with different membrane shapes and three different membrane materials- silicon nitride, polyimide and SU-8. With the help of these simulation results, the right shape for the membrane and the right material for the membrane to address the above mentioned issues is identified. The fabrication procedure carried out and the results obtained along with their discussion are presented in the following sections.

5.2   Process steps employed to create the 3D model

- A substrate of certain thickness is considered and is used as the ground electrode
- A sacrificial is deposited to a thickness equal to the gap height required
- This layer is then patterned to create a circular cavity of required radius using a mask

- A layer of membrane material of required thickness is stacked over this patterned layer
- A thin layer of a metal is deposited over the membrane layer to act as the top electrode.

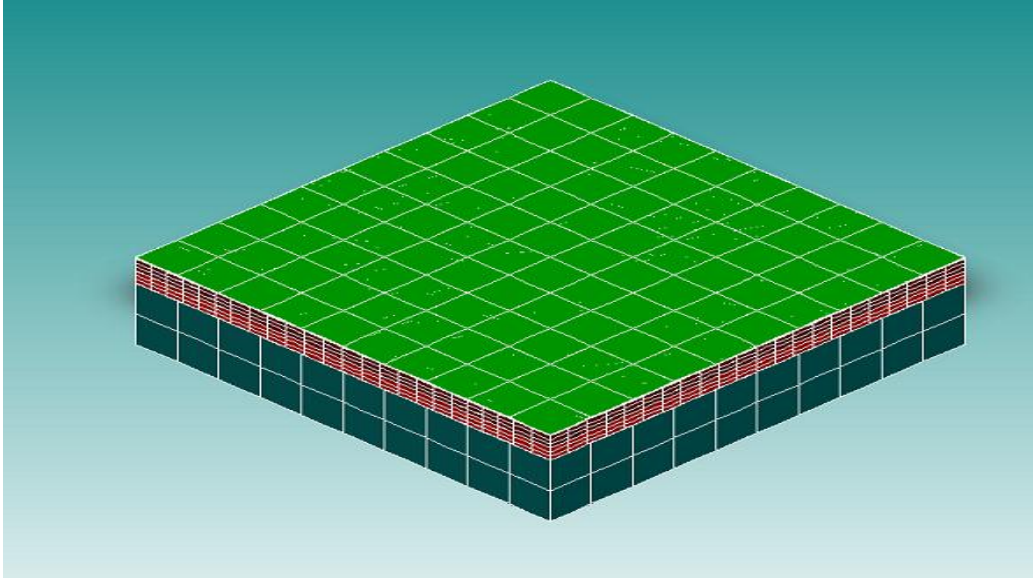A 3D model of CMUT created in CoventorWare looks as shown below.

Figure 5. 1: 3 D model of CMUT

5.3 Simulation of CMUTs with different membrane shapes

CMUTs can have membranes of different shapes- circular, hexagonal, square or rectangular. Keeping the area of gap constant, CMUTs are designed with circular, square and hexagonal silicon nitride membranes. Simulations are carried out on these CMUTs to identify the right shape that can be used.

Initially a circular CMUT is made with a cavity of radius 30um and thickness 1um. The area of this cavity is given by,

Area= $\pi r^2 = 2.8274E\text{-}09 \text{ m}^2$

For the same area, square and hexagonal shaped cavities were formed. The length of the sides for this area was calculated to be 53.174um for square cavity and 32.98um for hexagonal cavity.

Simulations were carried out on these by applying atmospheric pressure load and voltages of 50V and 400V. The corresponding deflections were noted. The natural frequency was also determined by performing a modal analysis. Through pull in analysis, the collapse voltage was determined. The results are shown in Table 5.1. As can be seen from the above table, circular membranes yield the highest displacement for a given load. With respect to area efficiency, while making arrays, hexagonal and square membranes yield the best results.

Membrane shape	Static capacitance (fF)	Disp for 0.1MPa (nm)	Disp for 50V (nm)	Disp for 400V (um)	Natural frequency (MHz)	Pull in voltage (V)
Circular	66.3	27.38	2.93	0.1402	5.8458	550
Square	65.98	21.588	1.4679	0.1046	6.602062	695
Hexagon	65.72	25.812	1.74235	0.128	6.027792	631

Table 5.1: Simulation results on CMUTs with different membrane shapes

5.4 Simulation of CMUTs with different membrane materials

CMUTs with different materials- silicon nitride, SU-8, polyimide were designed for a natural frequency of 50kHz using the design formula mentioned in Section 3.6. The properties of these materials and dimensions chosen for 50kHz operation are listed in Table 5.2. A 1um aluminium layer is deposited to act as top electrode.

	Si_3N_4	Polyimide	SU-8
Young's modulus (E)	320GPa	2.5GPa	4.02GPa
Poisson's ration (σ)	0.263	0.34	0.22
Density (ρ)	3270	1420	1190
Membrane radius (a)	1mm	260um	460um
Thickness (d_m)	10um	5um	12um
Gap height (d_0)	10um	5um	2um

Table 5.2: Membrane material properties and dimensions used for simulation

5.4.1 Simulation Results

Pressure loads and voltages applied on these CMUTs yielded the displacements (in um) as shown in Table 5.3.

Load applied	Si_3N_4	Polyimide	SU-8
Natural frequency	58.9kHz	107kHz	81kHz
0.01MPa	3.3233	3.18	3.8
0.1MPa	16.61	10	19.4
50V	2.614e-02	0.1266	0.485
Pull in voltage	520	140	75

Table 5.3: Displacements with different loads applied

The above displacements were obtained with devices of different dimensions and gap size. For better visualization of advantages of SU-8 over silicon nitride, a silicon nitride CMUT was made with same dimensions as Su8 above. Results are shown in Table 5.4:

Load applied	Si_3N_4	SU-8
0.01MPa	0.149	3.8
0.1MPa	1.49	19.4
50V	0.16363	0.485
150V	0.28	4.1453

Table 5.4: Displacements of different membrane CMUTs with same dimensions

5.4.2   Conclusion

From the above results, we see that with silicon nitride, low voltage operation is not possible. Though silicon nitride membranes have lesser displacement under atmospheric pressure, they need high voltages for their operation. Hence polymers- polyimide and SU-8 are good options. SU-8 is chosen because of ease of fabrication and high yield strength.

5.4.3   About SU-8

SU-8 is a photoresist used commonly for thick-film MEMS applications. It is a negative photoresist and can itself act as sacrificial layer. It is a low cost, user friendly material and can be made into molds. The present application requires a thick membrane material that enables low voltage operation, that sustains large deflections due to atmospheric pressure plus the applied voltages and that enables fabrication of large devices easily and inexpensively. SU-8 has been found to been found to be a very attractive material suited for this application. Its low Young's modulus enables low voltage operation at low frequencies. Also, the frequency of operation is chosen close to resonance thus further increasing displacements at low voltages. Further, because of its large yield strength, it can be operated as a CMUT even after large displacements due to atmospheric pressure while use in air.

While using it to fabricate CMUT, a thick layer of SU-8 can be spun and only the required thickness is hardened by exposure to illumination. The rest will act as sacrificial layer and can be etched out. Hence gaps of more than 2um thickness can be created. On the other hand, if oxide is used as sacrificial layer with silicon nitride membrane, there is a limit on the oxide thickness that can be grown. Thus SU-8 helps solve this problem.

5.5   Transient and Harmonic Analysis

Atmospheric pressure causes considerable displacement of the membrane. This happens due to the pressure gradient that exists on either side of the membrane. This effect was thought

to be addressed by introducing air at a certain pressure in the gap to control the amount of displacement. To find the right pressure, simulations were carried out with 0.1MPa applied at top of the membrane and varying the pressure applied to bottom of membrane. For this, a silicon nitride CMUT with 100um radius and 0.5646um thick membrane was used. The resulting displacements are shown in Table 5.5

Pressure applied to bottom face of the membrane (MPa)	Displacement (um)
0.1	1.0843e-04
0.099	1.0438
0.098	1.6825
0.097	2.125
0.096	2.469
0.095	2.753

Table 5.5 : Displacements with pressure applied to bottom face of membrane

Air at pressures less than 0.098MPa is as good as vacuum in the gap. Hence only option to reduce displacement is to use 0.1MPa or 0.099MPa air in gap. Transient analysis is carried out by applying a 50V pulse without and with air of 0.099MPa to see the effect of air in gap. The results are shown below.
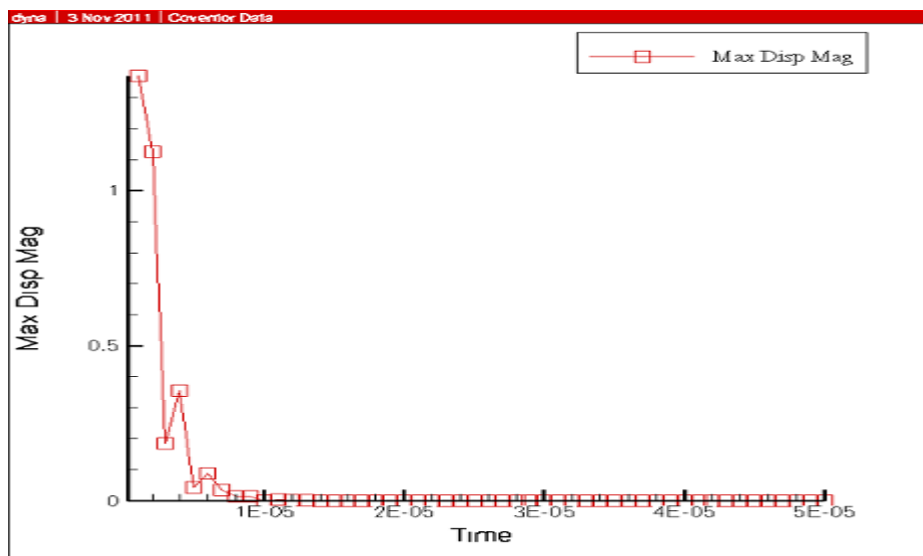
Figure 5.2: Transient response for a 50V pulse with vacuum filled cavity
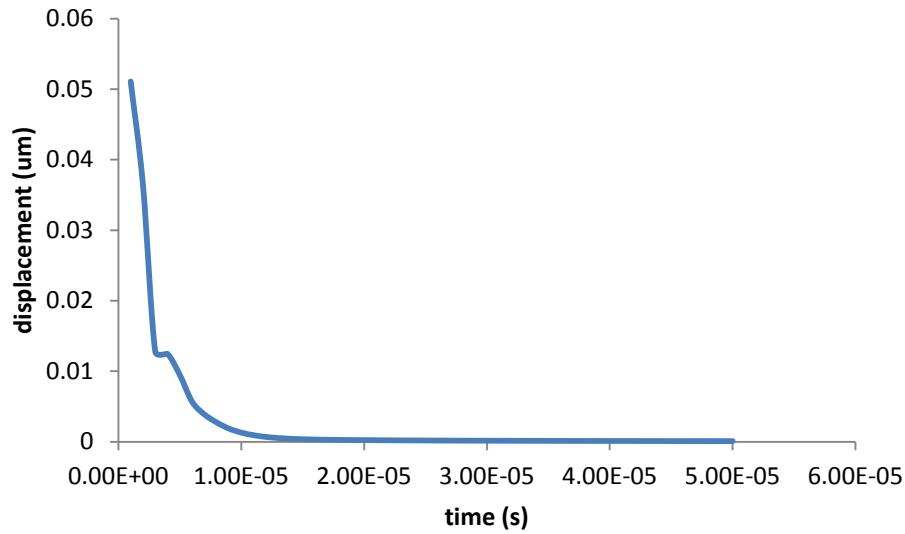
Figure 5.3: Transient with a 50V pulse with 0.099MPa air in gap

From the transient results, it is seen that with air in the gap, displacements of the membrane are drastically reduced than in the case with vacuum in the gap. If we fill the gap with air, deflections due to air pressure may reduce, but the achievable displacements due to applied loads also reduce. Thus we have to increase voltages applied to achieve the same displacements as with vacuum. This is not feasible for the present application. Hence, the option left is to create large gaps, let the membrane displace due to air pressure and then use it for normal operation as a transducer for ultrasound generation and reception.

Next harmonic analysis was performed on the CMUT with SU-8 membrane with dimensions mentioned in Table 5.2 . Here a DC voltage is applied and over it a sinusoidal signal of small amplitude is superimposed and the frequency response is determined over the desired range of frequencies. For a DC of 50V, 100V, 120V and 150V and a superimposed AC of 20mV, the frequency responses obtained are as shown below.
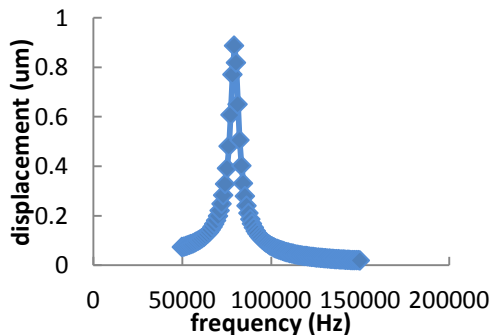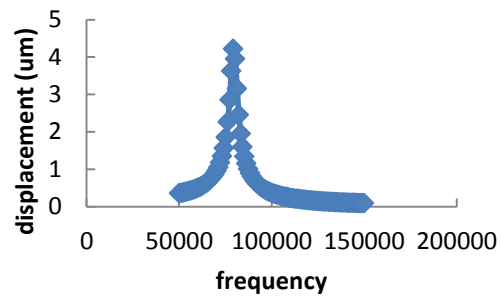

(a). DC=50V and AC=20mV

(b). DC=100V, AC =20mV

37
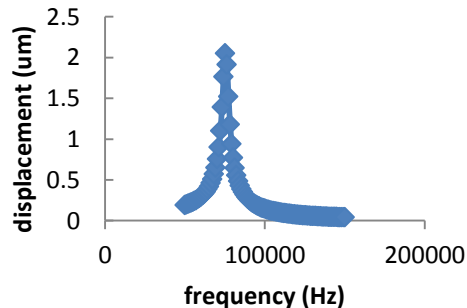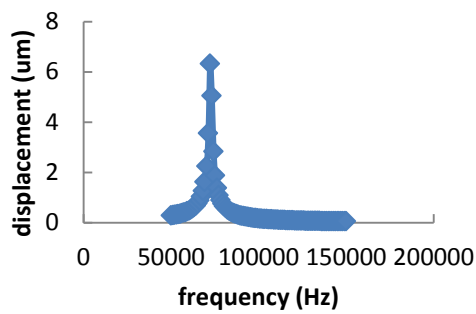
(c). DC=120V,AC=20mV   (d). DC=50V, AC=100mV

Figure 5.4: Frequency responses with various DC and AC applied

Through these results, effect of electrostatic spring softening is seen. The resonant frequency decreases with increase in applied DC voltage. Also, due to resonant phenomena large displacements are achievable at frequencies close to resonance frequency. If the DC is kept constant and AC increased, then the displacements at respective frequencies are also increased as can be seen in the plots (a) and (d). Next harmonic analysis is carried out with a DC of 22V, a limit on DC voltage that can be carried by a person. The response is shown in Figure 5.5.
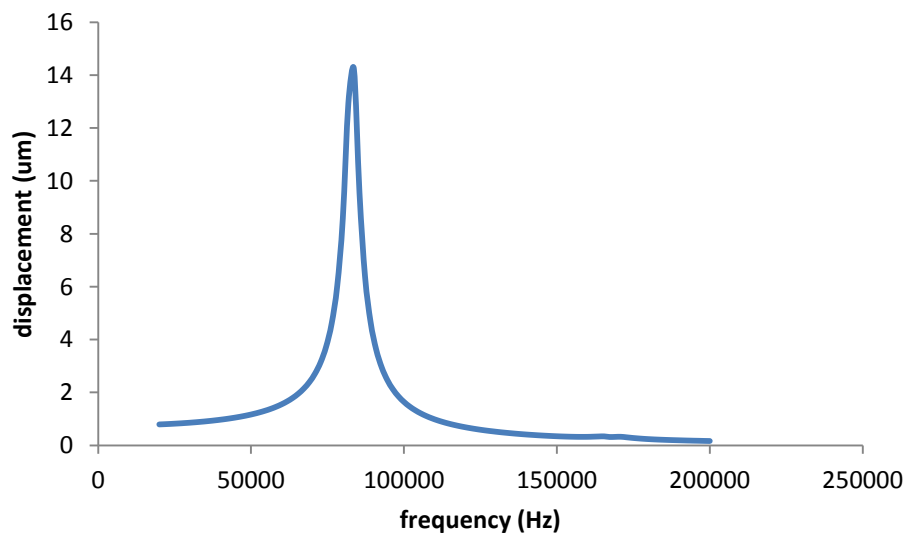
Figure 5.5: Frequency responses with DC of 22V and AC of 0.5V

We see that for the CMUT with 2um gap, displacements close to 2um is obtained at around 51kHz with a small DC applied.

Chapter 6

6.   Transmitter Design

The transmitter generates ultrasound when subjected to a DC and an AC voltage. The displacements of the membrane should be large to create large disturbances in the surrounding air so that the resulting ultrasound can travel long distances. Through simulations results presented in the previous chapter, CMUTs with circular membrane and SU-8 as membrane material are thus desired as they help achieve large displacements. Ultrasound attenuates rapidly in air and this attenuation increases with frequency. Hence CMUT needs to be designed for low frequency operation. As seen in Eq. 6, we can have membranes with different radius and thickness while keeping the ratio $\dfrac{d_m}{a^2}$ constant. But devices with small radius and small membrane thickness break down when exposed to atmospheric pressure. Hence we have to use devices with large radius and membrane thickness to sustain this defection.

With the above considerations, a transmitter is designed with the following dimensions for 50kHz operation.

Membrane radius: 460um

Membrane thickness: 12um

Gap thickness: 5um

Top electrode thickness: 1um

6.1   Transmitter Simulations

Static simulations on the transmitter carried out in CoventorWare yielded the results shown in Table 6.1.

Natural Frequency	80.568kHz
0.1MPa load	20um displacement
0.01MPa	3.81um displacement
100V	0.31um displacement
Pull in voltage	~242V

Table 6.1: Static simulation results of transmitter

Though the membrane dimensions are chosen for 50kHz operation, the natural frequency is found to be 80kHz. This is because on depositing a metal electrode over the SU-8 membrane, its stiffness increases thereby increasing the natural frequency of the membrane metal combination.

Since 20um displacement happens due to atmospheric pressure, the CMUT should be made with 25um gap so that 5um remains for normal operation. To ensure that Su8 can sustain this large displacement, increasing pressures were applied to the membrane. When applied load is too high, simulation in CoventorWare fails. The results obtained is shown in Table 6.2.

Pressure	Displacement
0.1MPa	20um
1MPa	48.7um
5MPa	86.46um
10MPa	110.8959um
20MPa	143.123um
40MPa	187.26um
50MPa	failed

Table 6.2: Displacements with increasing pressure load

Thus displacements as large as 190um are possible with this membrane dimensions.

Next harmonic analysis is performed on the CMUT by applying 22V DC and 0.5V AC. The frequency response obtained is as shown in Figure 6.1. At 76kHz, displacement of 4.92um which is as large as the gap is obtained with just 22V DC applied!
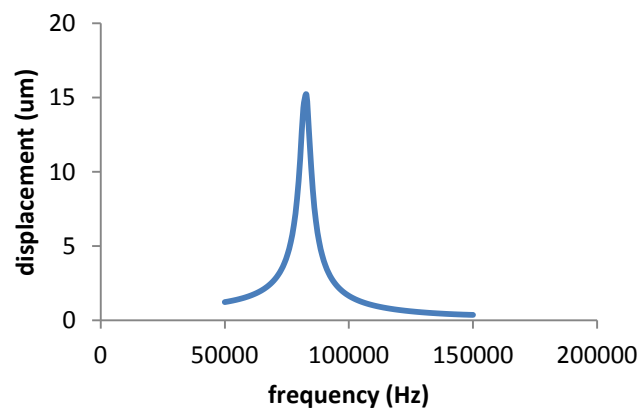
Figure 6.1: Frequency response of transmitter with DC=22V and AC=0.5V

6.2   Pressure Distribution of Transmitter

From harmonic analysis in CoventorWare, we have obtained a displacement of 4.92um at 76102.04082 Hz. Using this as a boundary condition in COMSOL, the pressure output from the CMUT is determined. It is found to be 140.3dB on the surface. The pressure distribution around a 1mm sphere in terms of sound pressure level (SPL) is shown in Figure 6.2. At 1mm, the SPL is 118dB.

From theoretical calculations, the SPL at 2m is determined. Using the formula for free field propagation of sound in air, we can find the attenuation for this distance. Attenuation of sound when it travels a certain distance away from a reference distance is given by

$$L_{p1} - L_{p2} = 20\log(\frac{r_2}{r_1})$$

Eq. 8

Where $L_{p1} - L_{p2}$ = difference is SPLs of that at reference distance and that at desired distance

r_2 is the distance at which SPL is to be calculated = 2m

r_1 is the reference distance= 1mm

Using the above values we get the difference to be 66.021dB

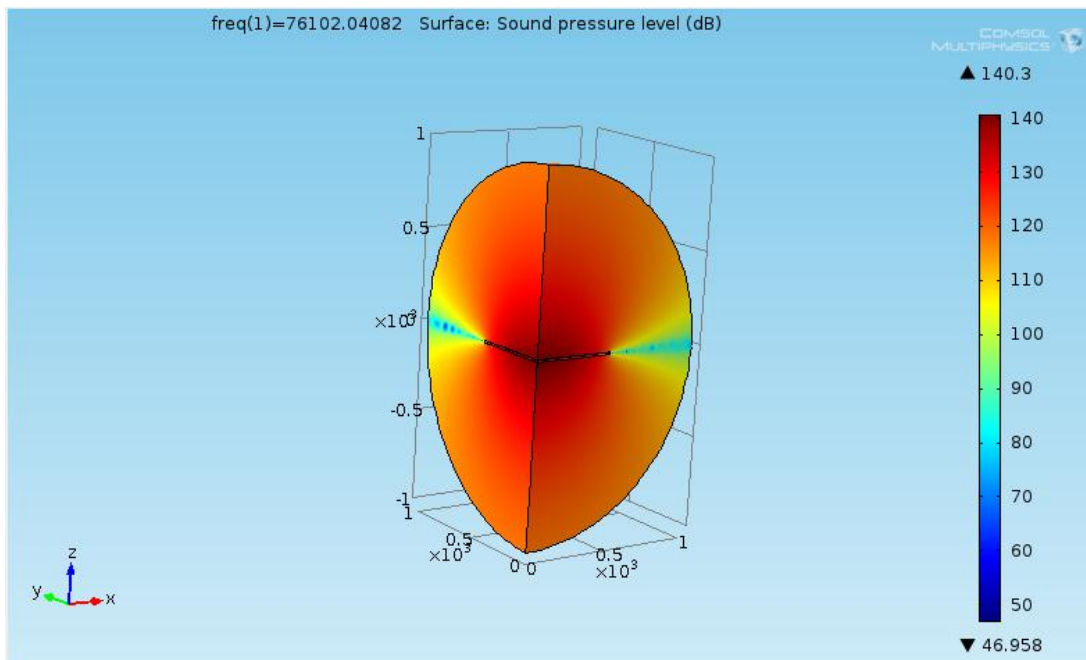In addition, there is also frequency dependent attenuation given by,

Figure 6.2: Sound Pressure Level distribution of the CMUT

$L = 0.022 f - 0.6$ dB/ft   Eq. 9

where f= frequency in kHz

For f =76102.04082Hz, L = 1.074dB/ft = 3.524dB/m.

For 2m, L= 7.05dB

Thus total loss T = 73.068dB.

At 2m, the SPL is thus 118-73.068= 44.932dB

We now know the SPL of sound that reaches the object to be detected. Depending on the reflection coefficient of object to sound, only a part of this is reflected. The reflection coefficient is calculated as,

$$R = \left(\frac{Z_2 - Z_1}{Z_2 + Z_1} \right)^2$$ Eq. 10

where Z_2 and Z_1 are the acoustic impedances of the two media where sound is incident and sound reflects back into.

　　　Typical objects that can be encountered by the blind in the environment being considered will be made of materials like wood, steel, aluminium, concrete etc. The acoustic impedances of these materials is calculated as

$$Z = \sqrt{E\rho}$$ Eq. 11

where E= Young's modulus of the material, ρ = density of the material

The acoustic impedances of these materials is shown in the Table 6.3. The acoustic impedance of air is just 415Rayls. Since the impedances of target materials is very high, reflection coefficient is as high as 0.999. Thus the SPL of reflected sound is 44.932dB. Received signal at the transducer will thus be 44.932-73.068= -28.136dB which is 0.784uPa.

Material	E (GPa)	ρ (kg/m^3)	Z (MRayls)
Wood	11	510	2.37
Aluminium	69	2700	13.65
Steel	200	7850	39.62
Concrete	30	2400	8.51

Table 6.3: Acoustic impedances of some materials

　　　Simulation is also carried out using a 2mm sphere. At 2mm, the SPL is found to be 111dB which is approximately 6dB less than that at 1mm. This directly follows from the Eq. 8 that on doubling of distance, SPL reduces by 6dB. When an array of four transducers

placed in the form of 2*2 array is used, the SPL distribution obtained is shown in Figure 6.3.
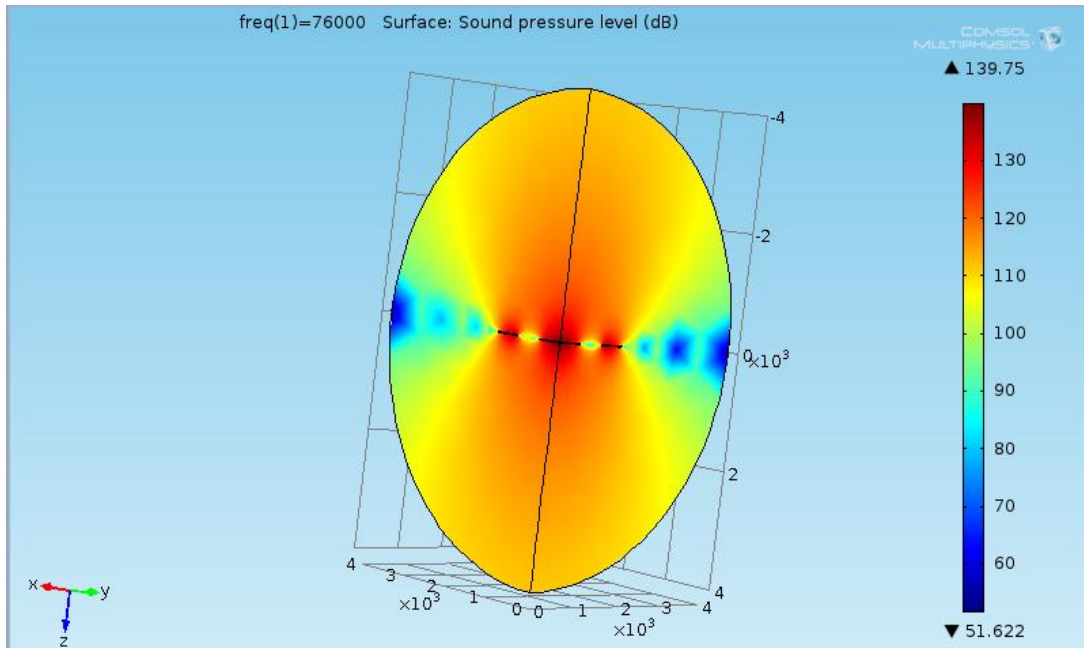

Figure 6.3: SPL distribution for an array of four transducers

For this simulation, a 4mm sphere is used. The SPL at 1mm is 120.85dB, 116.55dB at 2mm, 113.74dB at 3mm and 111.49dB at 4mm. Around 3dB increase in SPL is found with the above arrangement. Also, with doubling of distance, the decrease in SPL is less than 6dB.Thus it is shown that by using an array of transducers, the SPL can be increased.

Chapter 7

7. Receiver Design

The receiver receives ultrasound reflected from an obstacle and generates a proportional current. The receiver is biased at a DC voltage close to its pull in voltage. When an ultrasound signal impinges on the membrane, it produces capacitance changes resulting in proportional current being generated. Since ultrasound attenuation in air is high, the received signal will be very small. To detect this, a CMUT with light membrane and a small gap is required. Smaller the gap, higher is the receive sensitivity. As seen, on travelling a to and fro distance of 2m, the pressure received will be just around 1uPa. Assuming that using an array, a received pressure of 100uPa is achievable, a receiver CMUT with SU-8 membrane and a resonant frequency of 50kHz is designed with the following dimensions.

Membrane thickness – 0.5646um

Membrane radius – 100um

Gap height – 1um

Top electrode thickness – 0.01um

7.1 Receiver Simulations

Static simulations on the receiver carried out in CoventorWare yielded the results shown in Table7.1.

Natural Frequency	83.766kHz
0.1MPa load	7.75um displacement
0.1mPa	0.748pm displacement
0.005V	0.6635pm displacement
0.02V	10.62pm displacement
2V	0.121um displacement
3V	0.3293um displacement
Pull in voltage	~3.6V

Table7.1: Static simulation results of receiver

Though the membrane dimensions are chosen for 50kHz operation, the natural frequency is found to be around 83kHz. This is because, as in the case of transmitter, on

depositing a metal electrode over the SU-8 membrane, its stiffness increases thereby increasing the natural frequency of the membrane metal combination. The device has a displacement of 7.75um due to air pressure. Through simulations in CoventorWare similar to that carried out to obtain results presented in Table 6.2, the membrane is seen to tolerate a maximum of 15um displacement. Thus the device should be fabricated with a gap of 8.75um so that 1um remains after bending due to air pressure.

Harmonic analysis is then carried out by biasing the device at 3V and superimposing a 0.1V AC signal on it. The frequency response obtained is shown in figure below.
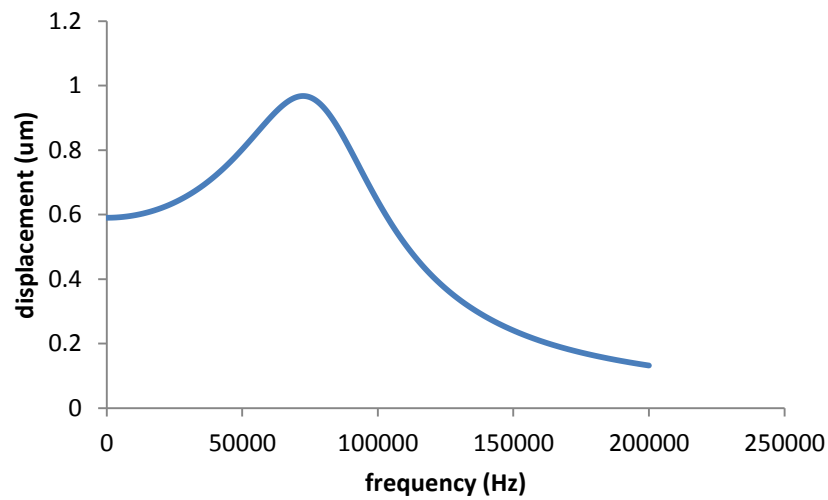
Figure 7.1: Frequency response of receiver CMUT with DC=3V and AC=0.1V

7.2   Output Current from Receiver CMUT

The output current from a CMUT biased at a certain DC when subjected to an ultrasonic wave is given by.

$$I_{CMUT} = V_{BIAS} \frac{C_0}{d_0} \frac{\partial d}{\partial t}$$
Eq. 12

To get an idea about output current, we thus need to obtain transient response of the biased CMUT to an incoming ultrasound wave. Since carrying out a transient analysis is very tedious and time consuming using simulators, a simpler approach is used that gives an approximate idea of generated current. The Inverse Fourier Transform of the harmonic response presented in Figure 7.1 is determined using MATLAB. This gives the impulse response of the system in um/V over time base as shown in Figure 7.2.
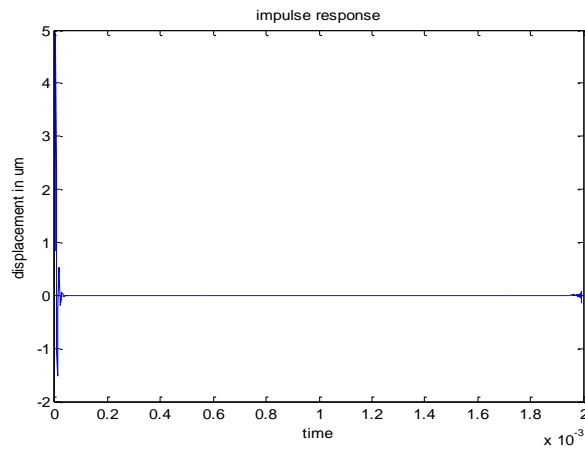
Figure 7.2: Impulse response of 3V biased receiver CMUT

We know that convolving the impulse response with any input gives the response of the system to that input. The same concept is used here. Since the pressure wave of 100uPa cannot be directly convolved with the impulse response which is in um/V, the DC voltage that gives almost the same static displacement as that of 100uPa is first determined. This value is found to be 0.005V. This signal at 76kHz is convolved with the impulse response. The resulting response is shown in Figure 7.3.
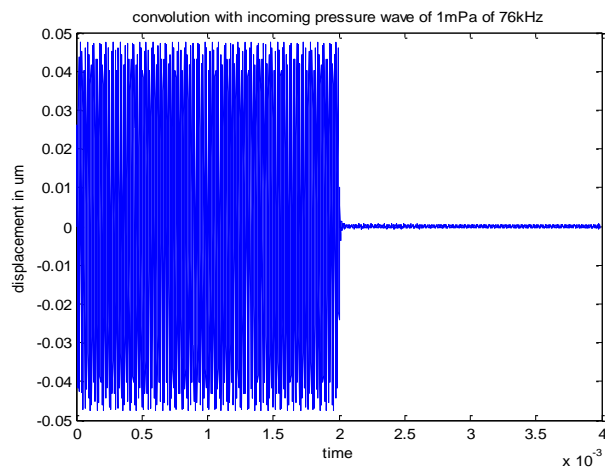
Figure 7.3: Response of receiver to 100uPa equivalent sine wave

Using arbitrary two consecutive values of the response, the current is found to be 15nA. Thus by using an array of receivers, a sufficient current for further processing can be generated.

Chapter 8

8.   Towards Fabrication

Through simulations, the validity of CMUTs for application in ETA is confirmed. Transmitter and receiver CMUTs have been designed to meet the needs of ETA for indoor navigation. The next step is thus the fabrication of these CMUTs and testing them by applying various loads to check if they match the results as obtained through simulations. The fabrication steps for these CMUTs that have been proposed and appropriate masks that have been designed are discussed in the following sections of the chapter.

8.1   Fabrication Steps

A four level mask fabrication process is proposed for making an array of tranducers on a complete 2 inch wafer. The steps for the fabrication of a single CMUT are shown below.

Step 1: Wafer cleaning - A 2 inch wafer (maroon layer) is considered and RCA cleaning is performed.

Step 2: Oxidation – Silicon di oxide (blue layer) of 400nm thickness is grown on the silicon substrate

Step 3: Deposition – 200nm thick gold (yellow layer) is deposited to act as the bottom electrode. This layer is then patterned using MASK 1.

Step 4: SU-8 spinning – 40um thick SU-8 (purple layer) is spun on the surface. For this thickness, the rate of spinning needs to be found by experimentation.


Step 5: Prebake – Prebake the spun SU-8 at 65^0C for 5 min and then increase the temperature to 95^0C and bake for 15 min

Step 6: Lithography – Using MASK 2, harden the exposed SU-8 (black layer) completely over 40um thickness.

(UV exposure)
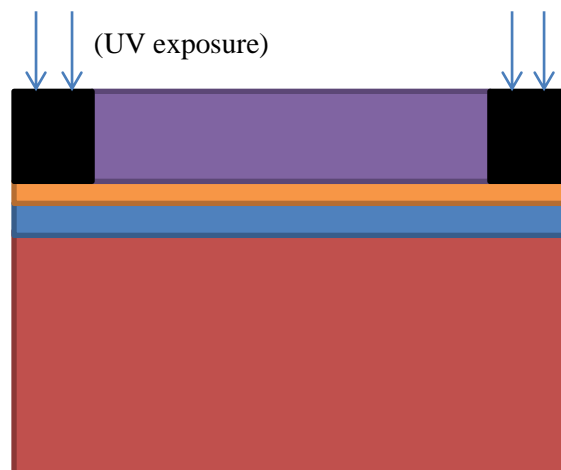
Step 7: Lithography – Using MASK 3, harden only 12um of circular portion in the centre. This acts as the membrane. A certain portion of SU-8 is left unhardened on the sides. This is to later remove the SU-8 below the membrane which acts as the gap.
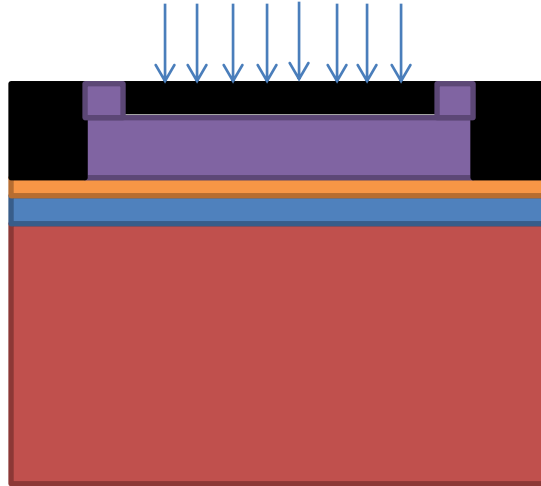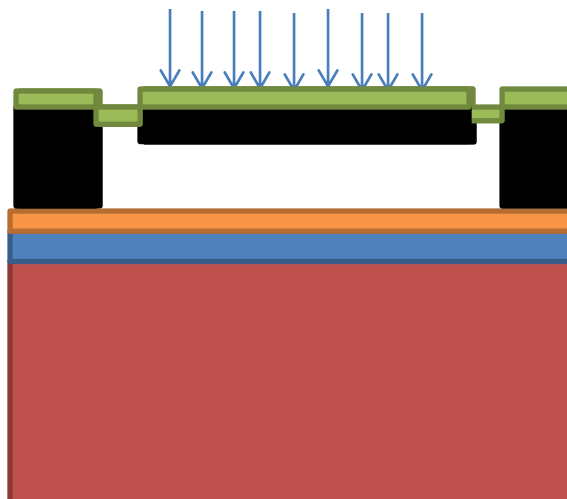
Step 8: SU-8 development- Remove the unexposed SU-8 using the developer

Step 9: Post bake - Bake the wafer at 65^0C for 1 min then slowly ramp to 95^0C and bake for 4 min.

Step 10: PPR spinning - Spin 1um of PPR (green layer). Using MASK 4, expose PPR in the area where gold is to be deposited.

Step 11: PPR Patterning and Gold Deposition - Later dip in chlorobenzene and use ultrasonic bath to remove this exposed PPR. Deposit gold of 1um thickness in these regions.

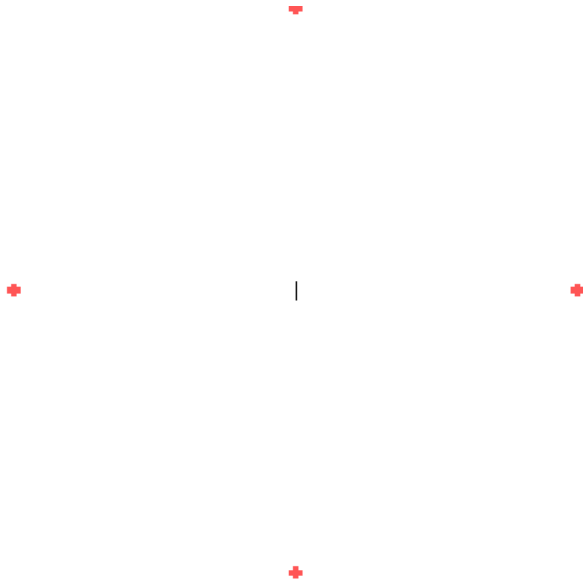Step 12: Lift off - Remove the remaining PPR using lift off

Thus a completely fabricated CMUT cell in side view looks as shown in the above figure.

8.2   Mask Layouts

As seen from the fabrication process, four masks are required. The masks are used to make an array of tranducers on the silicon 2 inch wafer. The appropriate masks have been designed using Ledit software and have been submitted in CEERI, Pilani for mask making.

MASK 1: This is a dark field mask that creates alignment marks on the gold layer which acts as bottom electrode. The alignment marks are created on the centres of four sides of the mask. These marks are used for aligning with the masks that will be used later on in the process.

MASK 2: This is a light field mask that is used to harden 40um thick SU-8 in the support region of every CMUT. The spacing between CMUTs is around 2mm. This mask also creates pattern for taking contact to the bottom electrode on the left and right ends of the mask.
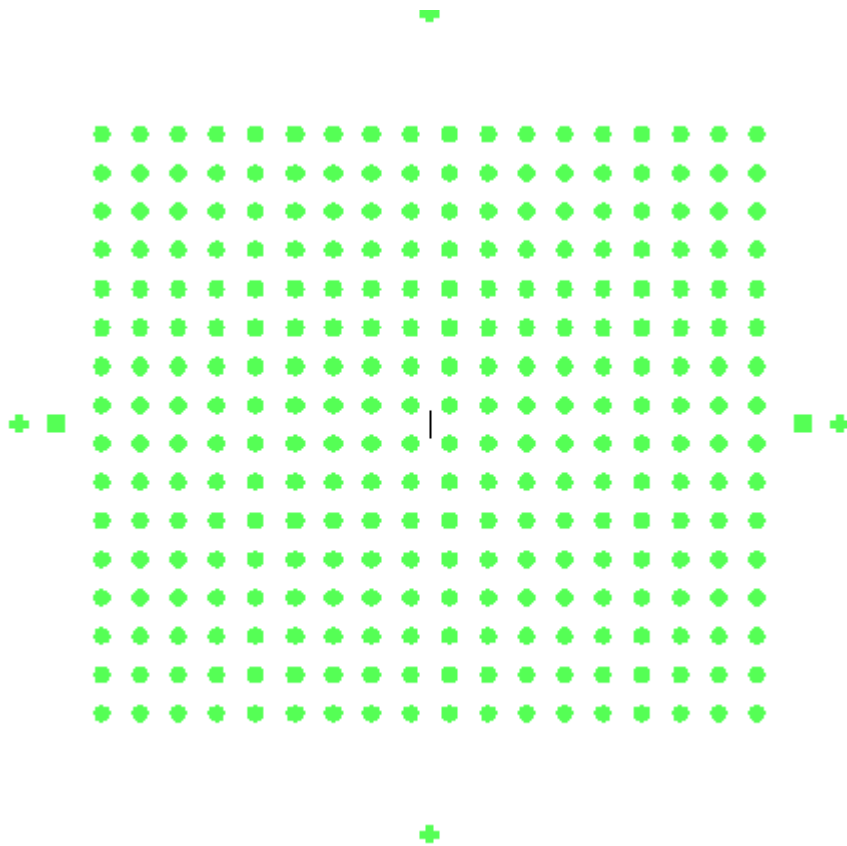
MASK 3: This is a light field mask and is used to harden only 12um in the circular portion of SU-8 that is left unexposed in the previous mask. A small region on the sides of every circular portion is left unexposed. This is required to remove the SU-8 below the 12um thick membrane SU-8 which forms the gap of the CMUT.

MASK 4: This is a dark field mask and is used to create a pattern for top electrode deposition.
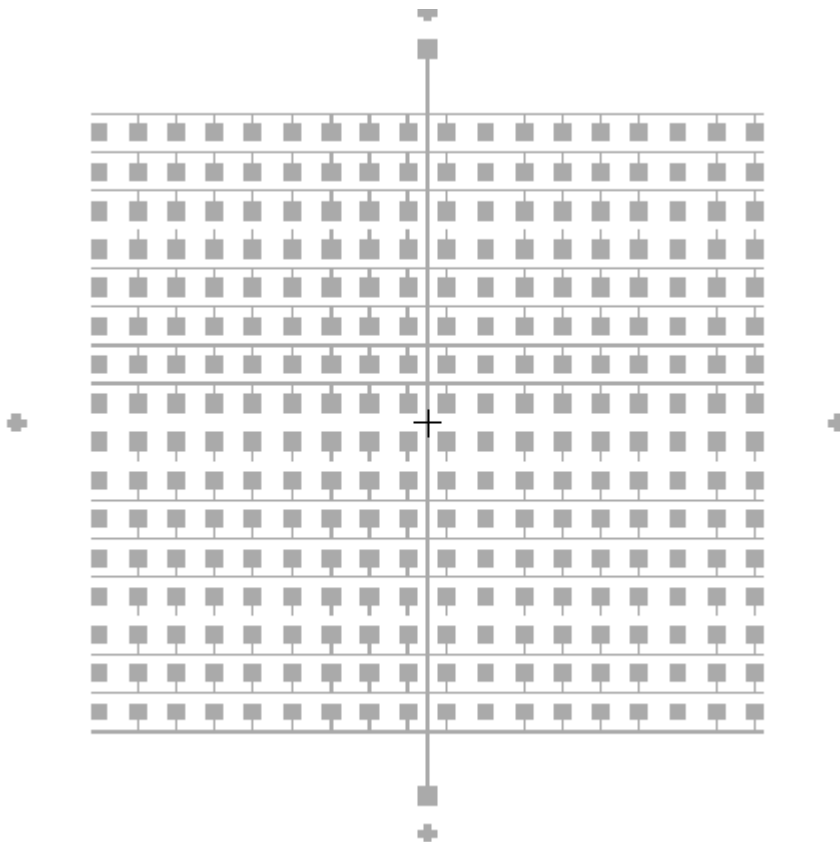
Chapter 9

9.   Generating actuation signal

After an obstacle has been detected, the distance of the obstacle from the user should be conveyed to the user. For this actuation signals in the form of vibration, electrostatic actuation etc are generally used. Here, a vibrator will be used to indicate the distance to the user. A vibrator has a motor over which an unbalanced load is present. Normally motors are well balanced and do not cause much vibrations. But on adding an unbalanced load, vibrations will be very high and proportional to speed of the motor. The speed of the motor is controlled by PWM signal. Hence a circuit to obtain this PWM signal needs to be designed which conveys information about distance of the obstacle. Such a circuit which derives a PWM pulse based on the time at which the received signal arrives at the receiver after transmission is developed and implemented off chip. To test the set-up, a peizoelectric ultrasound transmitter 255-400ST16-ROX and receiver 255-400SR16-ROX pair is used and operated at 40kHz.

The concept used here is to start up counting a counter when a burst of ultrasound is transmitted. The up count continues till a signal is received at the receiver. On reception of a signal at the receiver after encountering an obstacle, a circuit is used to derive a pulse from this received burst. This pulse is used to start down count of the counter. During the duration of down count till zero, a PWM pulse is obtained, the width of which gives distance information. This is later used to drive a vibrator. Thus, if the obstacle is far away from the user, the width of PWM pulse will be higher resulting in greater vibration intensity.

9.1   Circuit used to drive the transmitter

Ultrasound is generated from the transmitter as long as a drive signal is applied to it. Here, the requirement is to generate a burst of ultrasound of ten cycles. The next burst happens only after the received signal is received and processed. For testing purpose, the burst is emitted at fixed intervals. The circuit used to drive the ultrasound for burst emission is shown is Figure 9.1. An astable multivibrator is used to generate a square wave with an ON duration of 250us which corresponds to 10 cycles of 40kHz ultrasound. The OFF duration is chosen as 3ms which corresponds to the time taken by ultrasound to travel a to and fro distance of 1m assuming the range of these transducers is 0.5m. The output of astable multivibrator is labelled transmitted pulse (TP) and the falling edge of these pulses is used

to start up count of the counter. To obtain burst emission, an analog mux is used. One of the inputs is grounded and to the other, a 10Vrms 40kHz square wave is input. TP is used as the select signal. Thus the square wave reaches the transmitter only when TP is high resulting in burst emission.
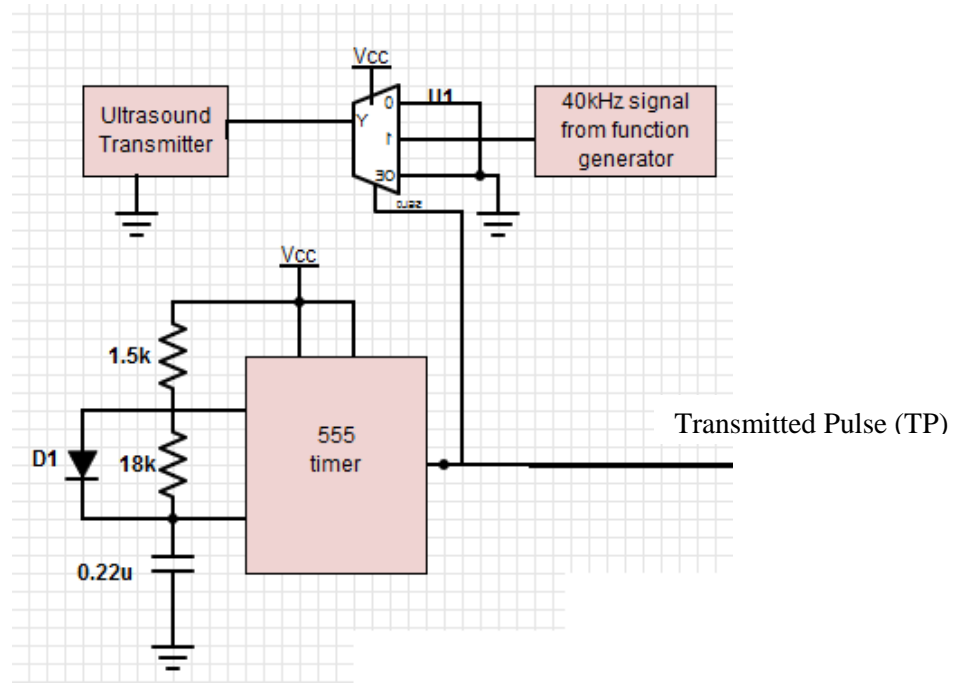

Figure 9.1: Transmitter drive circuit

9.2   Circuit used at the receiver to obtain a pulse from the received signal

The circuit used to obtain a pulse from the received signal is shown in Figure 9.2. This pulse is required to enable down count of the counter. The received signal is of very low value, around 200mV. It is given to a voltage follower and then amplified using a non-inverting amplifier with a gain of around 25 designed using CA3140E opamps. Gain higher than 25 cannot be obtained using these opamps because the gain bandwidth product of these opamps is around 1MHz. For a bandwidth of 40kHz, the maximum gain possible is thus 25. The amplified signal is passed through a peak detector circuit and a Schmitt trigger NAND gate IC 74132. This output is then inverted to obtain the receiver pulse (RP).

9.3   Circuit used to generate PWM pulse

The circuit used to obtain PWM pulse is shown in Figure 9.3. A power ON reset circuit generates a power on reset pulse (POR) that is used to reset all flip flops and counter in the circuit. On occurrence of TP, the T flip flop U4 toggles to high state thus making the counter count up. The counter has an inhibit pin that should be held low for normal operation of counter. Hence Qbar of U10 is given to this pin and this enables count

operation. When RP occurs from the receiver circuit, U4 toggles to low state thus making the counter to down count. During this interval, output of AND gate U8 also goes high. This output represents the PWM pulse. The output remains high till count goes down to zero. After zero count, to avoid the counter from underflowing and making the output of U8 high again, the falling edge of PWM pulse is used to change Qbar of U10 to high state. This inhibits count operation and the count remains at zero till the occurrence of TP which makes Qbar low.
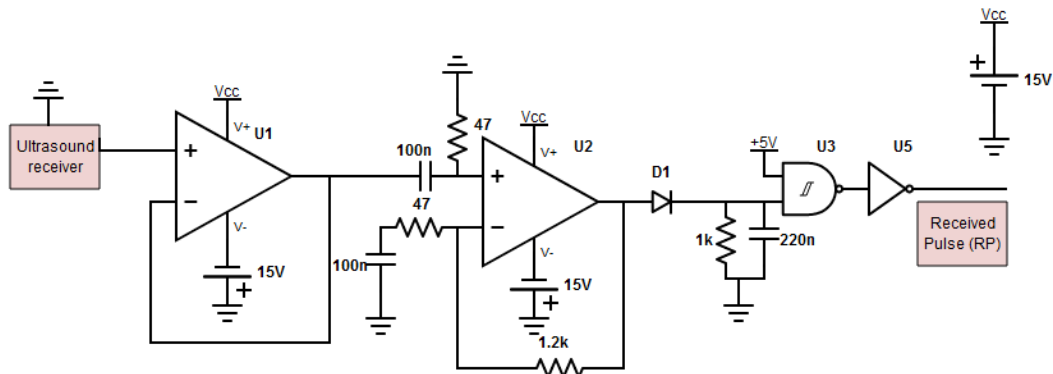

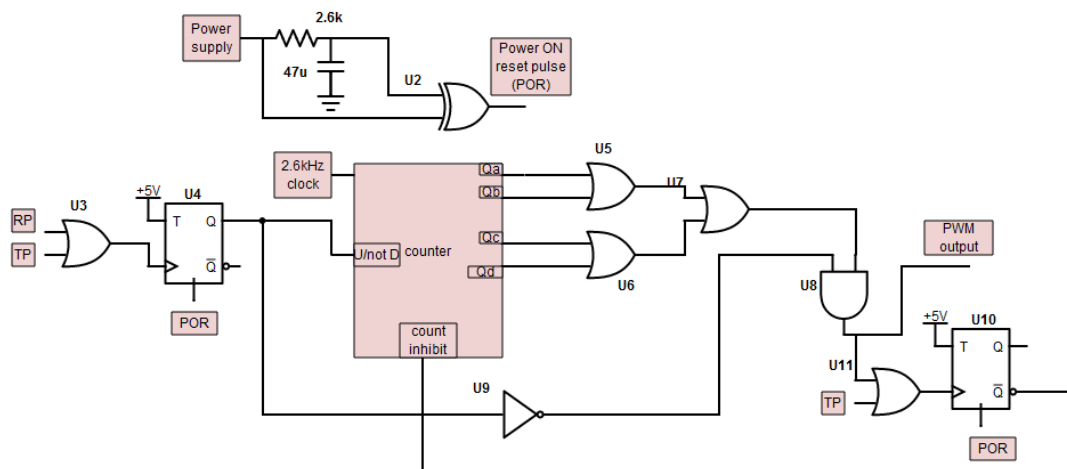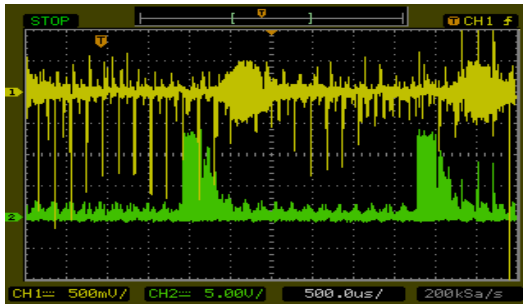Figure 9.2: Circuit used to obtain receiver pulse (RP)

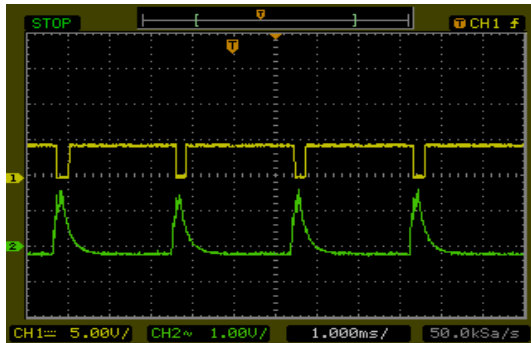Figure 9.3: Circuit to generate PWM pulse

9.4   Output waveforms

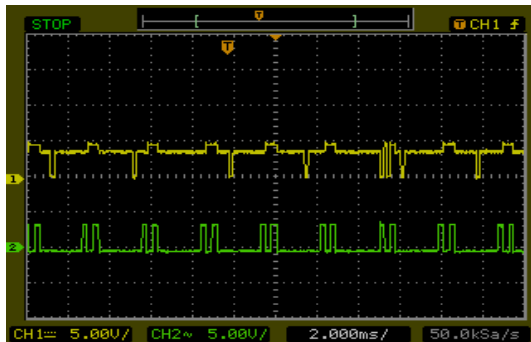The following are the waveforms obtained at various points of the circuit.

Green: Analog mux output to drive the transmitter to emit ultrasound burst.

Yellow: Received signal burst

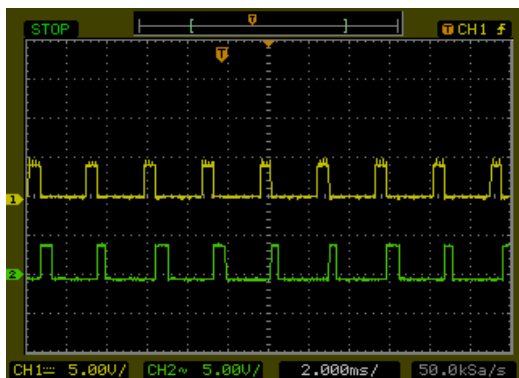Green: output of peak detector

Yellow: Output of Schmitt trigger

Green: output of OR gate U3- first pulse is TP and second is RP

Yellow: Output of OR gate U7- shows that after occurrence of RP down count starts and goes down to zero. This is obtained with inhibit pin grounded.

Yellow: Output of T flip flop- when output is zero, down count is enabled

Green: Output of AND gate U8 which is PWM output

References

[1] http://www.gizmag.com/go/3827/

[2] http://www.batforblind.co.nz

[3] J. Malvern Benjamin, "THE LASER CANE," *Journal of Rehabilitation Research and Development*

[4] J. Borenstein, "The NavBelt - A Computerized Multi-Sensor Travel Aid for Active Guidance of the Blind," Proceedings of the *CSUN's Fifth Annual Conference on Technology and Persons with Disabilities*, Los Angeles, California, March 21-24, 1990, pp. 107-116.

[5] Johann Borenstein, Iwan Ulrich, "The GuideCane — A Computerized Travel Aid for the Active Guidance of Blind Pedestrians," Proceedings of the *IEEE International Conference on Robotics and Automation*, Albuquerque, NM, Apr. 21-27, 1997, pp. 1283-1288

[6] Steven La Grow, "The use of the Sonic Pathfinder as a secondary mobility aid for travel in business environments: a single-subject design," *Journal of Rehabilitation Research and Development* Vol. 36 No. 4, October 1999

[7] Google books: Assistive Technology for Visually Impaired and Blind People by Marion A. Hersh

[8] Google books: Mobility training for visually handicapped people: a person centred approach by Allan Dodds

[9] www.singularityhub.com- The vOICE system rewires the brain's audio into visual.

[10] Ramiro Velázquez, Flavien Maingreaud and Edwige E. Pissaloux, "Intelligent Glasses: A New Man-Machine Interface Concept Integrating Computer Vision and Human Tactile Perception," *Proceedings of Eurohaptics*, 2003

[11] Sylvain Cardin, Daniel Thalmann and Frederic Vexo, "Wearable Obstacle Detection System for visually impaired People," *VR Workshop on Haptic and Tactile Perception of Deformable Objects*, p. p 50 – 55, 2005

[12] http://readperiodicals.com/201001/2019750381.html

[13] http://www.sensorsmag.com/sensors/acoustic-ultrasound/mems-reshapes-ultrasonic-sensing-1066

[14] Goksen G. Yaraliogly Arif S. Ergun, Yongli Huang, and Butrus T. Khuri-Yakub, "Capacitive Micromachined Ultrasonic Transducers for Robotic Sensing Applications," *Proceedings of the 2003 IEEE/RSJ InU. Conference on Intelligent Robots and Systems*, Las Vegas, Nevada ' October 2003

[15] Hideyasu SUMIYA, "Distance Feedback Travel Aid Haptic Display Design," Chapter 3, Mobile Robots: Perception & Navigation

[16] Jay P. Warren, Lisa R. Bobich, Marco Santello, James D. Sweeney, "Receptive Field Characteristics Under Electrotactile Stimulation of the Fingertip," *IEEE Transactions On Neural Systems And Rehabilitation Engineering*, Vol. 16, No. 4, August 2008

[17] Sakmongkon Chumkamon, Peranitti Tuvaphanthaphiphat, Phongsak Keeratiwintakorn, "A Blind Navigation System Using RFID for Indoor Environments," *Proceedings of ECTI-CON,* 2008

[18] Mohsin Murad, Abdullah Rehman, Arif Ali Shah, Salim Ullah, Muhammad Fahad, Khawaja M. Yahya, "RFAIDE – An RFID Based Navigation and Object Recognition Assistant for Visually Impaired People," *International Conference on Emerging Technologies - ICET* , 2011

[19] Igal Ladabaum, Xuecheng Jin, Hyongsok T. Soh, Abdullah Atalar, Khuri Yakub, "Surface Micromachined Capacitive Ultrasonic Transducers," *IEEE transactions on ultrasonics, ferroelectrics, and frequency control*, vol. 45, no. 3, may 1998

[20] Microsystem Design by Stephen Senturia

[21] Goksen G. Yaraliogly Arif S. Ergun, Yongli Huang, and Butrus T. Khuri-Yakub, "Capacitive Micromachined Ultrasonic Transducers for Robotic Sensing Applications," *Proceedings of the 2003 IEEE/RSJ InU. Conference on Intelligent Robots and Systems,* Las Vegas, Nevada ' October **2003**

[22] Arif Sanlı Ergun, Yongli Huang, Xuefeng Zhuang, Omer Oralkan, G¨oksen G. Yaralıo˜glu, Butrus T. Khuri-Yakub, "Capacitive Micromachined Ultrasonic Transducers: Fabrication Technology," *IEEE transactions on ultrasonics, ferroelectrics, and frequency control*, vol. 52, no. 12, december 2005

[23] Butrus T Khuri Yakub, Omer Oralkan, "Capacitive micromachined ultrasonic transducers for medical imaging and therapy," *Journal Of Micromechanics And Microengineering*, J. Micromech. Microeng. 21 (2011) 054004 (11pp)

[24] Y. Huang, E. Hæggström, B. Bayram, X. Zhuang, A. S. Ergun, C. H. Cheng and B. T. Khuri-Yakub, "Collapsed Regime Operation of Capacitive Micromachined Ultrasonic Transducers based on Wafer-Bonding Technique," *IEEE Ultrasonic Symposium,* 2003

[25] Baris Bayram, Omer Oralkan, A. Sanli Ergun, Edward Hæggstr¨om, Goksen G. Yaralioglu, Butrus T. Khuri-Yakub, "Capacitive Micromachined Ultrasonic Transducer Design for High Power Transmission," *IEEE transactions on ultrasonics, ferroelectrics, and frequency control*, vol. 52, no. 2, February 2005

[26] Ira O. Wygant, Mario Kupnik and Butrus T. Khuri-Yakub, "Analytically Calculating Membrane Displacement and the Equivalent Circuit Model of a Circular CMUT Cell," IEEE International Ultrasonics Symposium Proceedings,2008

[27] Ayhan Bozkurt, Igal Ladabaum, Abdullah Atalar, Butrus T. Khuri-Yakub, "Theory and Analysis of Electrode Size Optimization for Capacitive Microfabricated Ultrasonic Transducers," *IEEE transactions on ultrasonics, ferroelectrics, and frequency control*, vol. 46, no. 6, november 1999

[28] G. Caliano , A. Caronti, M. Baruzzi, A. Rubini, A. Iula, R. Carotenuto, M. Pappalardo, "PSpice modeling of capacitive microfabricated ultrasonic transducers," Ultrasonics, Vol. 40, Issue 1-8, pp. 449-455, Elsevier Science

[29] Goksen G. Yaralioglu, Baris Bayram, and Butrus T. Khuri-Yakub, "Finite Element Analysis Of Cmuts: Conventional Vs. Collapse Operation Modes," *IEEE Ultrasonics Symposium,*2006

[30] M.F. Teng, A. J. Hariz, "Characterisation and Modelling of MEMS Ultrasonic Transducers," *Journal of Physics*: Conference Series 34 (2006) 949–954, *International MEMS Conference* 2006

[31] Mario Kupnik, Ira O. Wygant, and Butrus T. Khuri-Yakub, "Finite Element Analysis Of Stress Stiffening Effects In CMUTs," 2008 *IEEE International Ultrasonics Symposium Proceedings*

[32] Shailendra Kumar Tiwaril, B.S. Satyanarayana2, A. Gopalkrishna Pail, Kunal K. Trivedi3, Rahul N. Sl, Pratyush Sahayl, "Hexagonal Capacitance Micromachined Ultrasonic Transducer," Proceedings of the 2008 *International Conference on Computing, Communication and Networking* (ICCCN 2008)

[33] Wei You, Edmond Cretu, Robert Rohling, "Analytical Modeling of CMUTs in Coupled Electro-Mechano-Acoustic Domains Using Plate Vibration Theory," *IEEE Sensors Journal*, Vol. 11, No. 9, September 2011

[34] Chris Daft, Sam Calmes, Daniel da Graca, Kirti Patel, Paul Wagner and Igal Ladabaum, "Microfabricated Ultrasonic Transducers Monolithically Integrated with High Voltage Electronics," 2004 *IEEE International Ultrasonics, Ferroelectrics, and Frequency Control* Joint 50th Anniversary Conference

[35] Ulkuhan Guler, Ayhan Bozkurt, "A Low-Noise Front-End Circuit for 2D cMUT Arrays," 2006 *IEEE Ultrasonics Symposium*

[36] Ira O. Wygant, Xuefeng Zhuang, David T. Yeh, Omer Oralkan, A. Sanli Ergun, Mustafa Karaman, Butrus T. Khuri-Yakub, "Integration of 2D CMUT Arrays with Front-End Electronics for Volumetric Ultrasound Imaging," *IEEE transactions on ultrasonics, ferroelectrics, and frequency control*, vol. 55, no. 2, February 2008

[37] Gokce Gurun, Paul Hasler, F. Levent Degertekin, "Front-End Receiver Electronics for High-Frequency Monolithic CMUT-on-CMOS Imaging Arrays," *IEEE Transactions on Ultrasonics, Ferroelectrics, and Frequency Control*, vol. 58, no. 8, August 2011

[38] Rudra Pratap, A Arunkumar, "Material selection for MEMS devices", *Indian Journal of Pure and Applied Physics*, Vol. 45, April 2007, pp. 358-367

[39] V. T. Srikar, S. Mark Spearing, "Materials Selection in Micromechanical Design: An Application of the Ashby Approach," *Journal Of Microelectromechanical Systems*, Vol. 12, No. 1, February 2003